

# Draft of the 2nd year review

29th June 2011

## Contents

<b>1</b>	<b>Introduction</b>	<b>2</b>
1.1	Localisation microscopy . . . . .	2
1.2	PALM, STORM . . . . .	2
1.3	Quantum dots . . . . .	2
1.4	Localisation microscopy using Quantum Dots . . . . .	3
1.5	Non-negative matrix factorisation . . . . .	3
1.6	Comparison NMF to the Richardson Lucy deconvolution . . . . .	3
<b>2</b>	<b>Model comparison problem</b>	<b>5</b>
2.1	Gamma Poisson (GaP) model . . . . .	5
2.2	Variational treatment of the GaP model . . . . .	6
2.3	Analysis of the residuals . . . . .	7
2.4	Results . . . . .	8
<b>3</b>	<b>Theoretical limits of the LM</b>	<b>12</b>
3.1	Cramer Rao bound . . . . .	12
3.2	Fundamental resolution measure (FREM) . . . . .	12
3.3	An alternative derivation of the FREM . . . . .	12
3.4	FREM for blinking sources . . . . .	14
3.5	Simulations . . . . .	15
3.6	Conclusions . . . . .	15
<b>4</b>	<b>Out of focus PSF</b>	<b>16</b>
4.1	Results . . . . .	16
<b>5</b>	<b>Conclusion and Future work</b>	<b>18</b>
5.1	Time series . . . . .	18
5.2	Future work and direction of the project . . . . .	18
	<b>References</b>	<b>19</b>
<b>A</b>	<b>NMF as a minimisation of Kullback–Leibler divergence</b>	<b>22</b>
<b>B</b>	<b>Variational approximation for GaP model</b>	<b>22</b>
<b>C</b>	<b>Resolution limit for the blinking QDs</b>	<b>28</b>

**Outline & summary** The second year review report summarises work on my PhD project I have done since September 2010. Section 1 gives a short introduction to localisation microscopy methods and is put into context of the recent research. Section 2 refers to the problem of the model selection. Theoretical limits of the localisation microscopy are discussed in Section 3. Section 4 demonstrates ability of the NMF algorithm to separate sources with different PSFs.

# 1 Introduction

## 1.1 Localisation microscopy

Localisation microscopy (LM) provides a conceptually simple way to super-resolution microscopy as a single source can be localised with an uncertainty much smaller than a classical Rayleigh’s resolution criterion (approximately  $\lambda_{em}/2$ , where  $\lambda_{em}$  is an emission wavelength of the source [Rayleigh, 1896, Born et al., 1975]). The Rayleigh’s criterion neglects the stochastic nature of the photon-detection process and does not take the total photon count (intensity of the source) into account. As shown in [Thompson, 2002, Ram et al., 2006b] the variance of a single source localisation is inversely proportional to the number of photons we can collect from this source. For sufficiently intense sources the localisation precision can significantly surpass the Rayleigh resolution limit [Gordon et al., 2004, Qu et al., 2004, Lidke et al., 2005, Ober et al., 2004].

## 1.2 PALM, STORM

In the real biological samples the sources are usually dense and highly overlapping. This prevents them from the individual localisation. PALM (Photo Activation Localisation Microscopy) [Hess et al., 2006] and STORM (STochastic Optical Resolution Microscopy) [Bates et al., 2007] separate the individual emitters by activating only a small subset of them at a time. If the activated subset is small enough the individual fluorophores are well spatially dispersed and the individual sources can be identified and localised. This requires a control of the sources activation/excitation. It can be achieved either by using photo-activable (PA) fluorophores (PALM, STORM) or by reversible photo - bleaching [Baddeley et al., 2009]. Repetition of this activation - localisation cycles can provide super-resolution images of biological samples [Shroff et al., 2008, Huang et al., 2008].

## 1.3 Quantum dots

Quantum dots (QD) represent an order of magnitude brighter and several orders of magnitude more photo-bleaching resistant fluorophores compared to the organic dyes used in LM [Jaiswal and Simon, 2004, Michalet et al., 2005]. QDs also provide a wide absorption and a narrow excitation spectrum which is very convenient for multicolour imaging. All these properties make QD very attractive for the biological research.

Under a continuous excitation QDs exhibit a blinking behaviour (fluorescence intermittency). They switch between “ON” episodes ( $1/\tau_{ON}^m$ ) of a rapid absorption-fluorescence cycling and “OFF” episodes ( $1/\tau_{OFF}^m$ ) where no light is emitted despite the continuous excitation. Both ON-time and OFF-time probability densities follow an inverse power law  $P(\tau_{ON/OFF}) \propto 1/\tau_{ON/OFF}^m$  [Kuno et al., 2001, Stefani et al., 2009]. However, the blinking process is not yet fully understood .

Despite all the advantages the QD can potentially provide, they are not suitable for the standard LM methods (PALM/STORM). The QD blinking behaviour is difficult to control and the overlapping sources cannot be separated and localised individually.

## 1.4 Localisation microscopy using Quantum Dots

In 2005 there has been published a method exploiting the fluorescence intermittency ('blinking') of QDs under continuous excitation [Lidke et al., 2005]. A time series of the blinking QDs was recorded and analysed using Independent Component Analysis (ICA) (FastICA algorithm [Hyvärinen and Oja, 2000] has been used). Localisation of two quantum dots separated down to 23 nm (corresponding to  $\lambda_{\text{em}}/30$ ) has been reported [Lidke et al., 2005]. Further exploration of the technique for more than two sources and for different configuration of the experiment can be found in [Lidke and Heintzmann, 2007].

A Bayesian approach to the blinking QD data has been presented in poster in 2008 [Harrington et al., 2008]. A model consisting of PSFs with known shape (all sources are assumed to have PSF of the same form) and individual intensities (normally distributed) was fitted to the data. Localisation of several QDs within the diffracted limited volume has been shown.

A method using QDs for measurement of sub-resolution distances has been published in [Lagerholm et al., 2006]. However, discrete ON-OFF blinking is required (only one source being ON and others OFF) as opposed to [Lidke et al., 2005, Harrington et al., 2008] where only fluctuation of the individual sources is needed.

## 1.5 Non-negative matrix factorisation

Non-negative matrix factorisation (NMF) seems to be a very natural model for describing the blinking QD data. The expectation value of noisy spatio-temporal  $N \times T$  data matrix  $D$  ( $N$  - total number of pixels,  $T$  - number of time slices) is assumed to be decomposed into the  $N \times K$  spatial component matrix  $W$  (images of the individual sources) and the  $K \times T$  temporal component matrix  $H$  (intensities of the sources).

$$\mathbb{E}[D] = \mathbb{E}[d_{xt}] = (WH)_{xt} = \sum_{k=1}^K w_{xk} h_{kt} \quad (1.1)$$

with non-negativity constraints  $d_{xt}$ ,  $w_{xk}$  and  $h_{kt} \geq 0$ .

The NMF algorithm shown in [Lee and Seung, 2001] minimises the Kullback-Leibler (KL) divergence between the data and the model. It can be shown that this is equivalent to the maximisation log-likelihood function of the model Eq (1.1) under the assumption of the Poisson noise (Appendix A). The details of the the algorithm are described in the first year review.

## 1.6 Comparison NMF to the Richardson Lucy deconvolution

An observed 'blurred' (diffraction limited) image  $I$  ( $N \times 1$  vector) can expressed as a (discretised) convolution

$$I_x = \sum_{j=1}^N W_j H_{x-j}$$

$W$  ( $N \times 1$ ) is the original (unblurred) object which represents locations and intensities of fluorescent sources.  $H$  ( $N \times 1$ ) is an image of point spread function (PSF) centred in the middle of the image Richardson [Richardson, 1972] and Lucy [Lucy, 1974] published an iterative deconvolution technique for astronomical images with known PSF. They used Bayes theorem as a 'hint' for an iterative update of  $W$ . This update is usually referred to as Richardson-Lucy (RL) deconvolution algorithm and is identical to the Lee-Seung NMF update with generalised KL-divergence objective function [Lee and Seung, 2001]. However, the matrices  $W$  and  $H$  represent different objects then in the NMF model. In the RL deconvolution one PSF is shared by all sources. In the NMF each source has its own PSF (columns of  $W$ ).

Holmes [Holmes, 1992] derived the RL updates based on maximum likelihood estimation of the model with Poisson noise using the expectation-maximisation algorithm. He also proposed an update for  $H$  so that the method can be used as a blind deconvolution algorithm (PSF is not known). They are sometimes referred to as a ‘blind RL algorithm’. The updates for  $W$  and  $H$  are technically identical to the Lee and Seung NMF updates (KL divergence as an objective function). Modified updates imposing radial symmetry constraints on PSF were also proposed.

There exist several modified updates derived using EM algorithm which impose some constraints on  $W$  or  $H$ . [Joshi and Miller, 1993] gives updates where Good’s roughness measure ( $\int \frac{|\nabla f(x)|^2}{f(x)} dx$ ) on the original image  $W$  is used as a regularisation term. This biases the solution towards the ‘smooth’ images and avoids speckle artefacts in the reconstructions that are sometimes experienced in deconvolution methods.

[Fish et al., 1995] use RL ‘blind’ algorithm (updates on both  $W$  and  $H$ ) but after some number of iterations they fit some approximation of the PSF to the estimated  $H$  and uses this fit as a new  $H$ . He claims that in noisy images this ‘semi-blind’ deconvolution can perform better than the one with known PSF.

The comparison of the rectified RL versions and some other deconvolution techniques has been shown in [van Kempen et al., 1997, Verveer et al., 1999]. RL usually performs well for noisy images.

## 2 Model comparison problem

NMF requires a prior knowledge about the number of components to be separated ( $K$  in Eq.(1.1) - rank of the factorisation). For noise-free data it is possible to estimate the number of sources by analysing principal components (PC), for example. However, in the noisy case the estimation of  $K$  is difficult.

The standard NMF algorithm maximises the likelihood of the model Eq.(1.1) under the assumption of the Poisson noise corrupted data (Appendix A). The likelihood function increases with higher  $K$  as the more flexible model fits the data better. The Bayesian Information Criterion (BIC) is a rough approximation of the Bayesian treatment penalising the complexity of the model. By evaluating the model for different values of  $K$  we can compare the BIC score. However, as shown in the first year review the BIC might be too crude approximation for the correct estimation of the data dimensionality.

A generative model underlying NMF is presented in section 2.1. A variational approximation for the Bayesian treatment of the problem (section 2.2) can provide estimation of  $K$  in the QD data.

A different approach to the model selection is shown in section 2.3. Analysis of the correlations in residuals (data-model) is used to estimate the number of components  $K$ .

These two different approaches have been applied to the simulated data with different densities of the sources. The results are shown in section 2.4.

### 2.1 Gamma Poisson (GaP) model

Gamma-Poisson (GaP) model [Canny, 2004] has been proposed as a probabilistic model for documents. It represents a generative probabilistic model for NMF Eq.(1.1). The entries  $h_{kt}$  (intensities of the sources) are treated as hidden variables generated from a Gamma distribution

$$p(h_{kt}|\alpha_k, \beta_k) = \frac{h_{kt}^{\alpha-1} \beta^\alpha \exp(-\beta h_{kt})}{\Gamma(\alpha)}$$

and the data  $d_{xt}$  modelled as a Poisson variable with mean  $\sum_k w_{xk} h_{kt}$

$$p(d_{xt}|w_{xk}, h_{kt}) = \frac{(\sum_k w_{xk} h_{kt})^{d_{xt}} \exp(-\sum_k w_{xk} h_{kt})}{d_{xt}!} \quad (2.1)$$

where  $w_{xk}$ ,  $\alpha_k$  and  $\beta_k$  are the parameters of the model.

The likelihood function of this model is given by

$$p(D, H|W, K, \theta) = \prod_{t=1}^T \prod_{k=1}^K p(h_{kt}|\alpha_k, \beta_k) \prod_{x=1}^N p(d_{xt}|w_{xk}, h_{kt}) \quad (2.2)$$

and the log-likelihood

$$\log p(D, H|W, K, \theta) = \sum_{t=1}^T \left\{ \sum_{k=1}^K \log p(h_{kt}|\alpha_k, \beta_k) + \sum_{x=1}^N \log p(d_{xt}|w_{xk}, h_{kt}) \right\}$$

The coupling between  $W$  and  $H$  in Eq.(2.1) prevents from integrating out the hidden variables  $H$  in Eq.(2.2) [Blei et al., 2003]. This is problematic as in the expectation maximisation (EM) algorithm [Bishop, 2006] it is necessary to evaluate the term  $\mathbb{E}_{h_{kt}} [\log \sum_k w_{xk} h_{kt}]$ . (In [Canny, 2004] a crude approximation is used  $\mathbb{E}_{h_{kt}} [\log \sum_k w_{xk} h_{kt}] \approx \log \mathbb{E}_{h_{kt}} [\sum_k w_{xk} h_{kt}]$ .)

## 2.2 Variational treatment of the GaP model

Variational treatment of the problem is proposed in [Buntine and Jakulin, 2006]. The detailed derivation is provided in Appendix B.

A new latent  $N \times K$  matrix  $V$  (entries  $v_{xk}$ ) is introduced such that

$$\sum_{x=1}^N v_{xk}^{(t)} = c_k^{(t)}$$

$$\sum_{k=1}^K v_{xk}^{(t)} = d_{xt}$$

where the discrete latent vector  $c_k$  gives the intensity of the  $k$ th component. The distribution of the underlying GaP model now becomes

$$h_{kt} \sim \text{Gamma}(h_{kt}; \alpha_k, \beta_k)$$

$$c_k^{(t)} \sim \text{Po}(c_k^{(t)}; h_{kt})$$

$$v_{x,k}^{(t)} \sim \text{Multinom}(v_{xk}^{(t)}; w_{xk}, c_k^{(t)})$$

and the likelihood of the GaP model with the latent matrix  $V$  is then

$$p(V, H | \alpha, \beta, W, K) = \prod_{t=1}^T \prod_{k=1}^K p(h_{kt} | \alpha_k, \beta_k) \prod_{x=1}^N p(v_{1k}^{(t)}, v_{2k}^{(t)} \dots v_{N,k}^{(t)} | h_{kt}, w_{xk})$$

$$= \prod_{kt} \text{Gamma}(h_{kt}; \alpha_k, \beta_k) \prod_x \text{Po}(c_k^{(t)}; h_{kt}) \times \text{Multinom}(v_{xk}^{(t)}; w_{xk}, c_k^{(t)})$$

explicitly

$$p(V, H | \alpha, \beta, W, K) = \prod_{kt} \frac{\beta_k^{\alpha_k} h_{kt}^{c_k^{(t)} + \alpha_k - 1} \exp(-(\beta_k + 1)h_{kt})}{\Gamma(\alpha_k)} \prod_x \frac{w_{xk}^{v_{xk}^{(t)}}}{v_{xk}^{(t)}!} \quad (2.3)$$

$D$  is derived from  $V$  ( $d_{xt} = \sum_k v_{xk}^{(t)}$ ) so it is not represented.

A factored posterior approximation is made for the latent variable to find expectations as part of an optimisation step.

$$p(V, H | \alpha, \beta, W, K) \approx q(V, H) = q_V(V)q_H(H) \quad (2.4)$$

where the optimal solution is given by [Bishop, 2006].

$$\log q_H^*(H) = \mathbb{E}_{V \sim q_V} [\log p(V, H, D | W, \alpha, \beta)] + \text{const}$$

$$\log q_V^*(V) = \mathbb{E}_{H \sim q_H} [\log p(V, H, D | W, \alpha, \beta)] + \text{const}$$

The likelihood of the data is bounded by

$$p(D | W, \alpha, \beta) \geq \mathcal{L}(q, W, \alpha, \beta) \quad (2.5)$$

where

$$\mathcal{L}(q, W, \alpha, \beta) = \mathbb{E}_{V, H \sim q(V, H)} [\log p(H, V, D | W, \alpha, \beta, K)] + C \quad (2.6)$$

is a variational lower bound [Bishop, 2006] and the constant  $C$  contains the entropy terms of  $q_H$  and  $q_V$  which are constant wrt  $W$ .

The factorised form Eq.(2.4) and the likelihood Eq.(2.3) suggest

$$q_H(H) = \prod_k \text{Gamma}(h_{kt}; a_k^{(t)}, b_k)$$

$$q_V(V) = \prod_{xk} \text{Mutlinom}(v_{xk}^{(t)}; n_{xk}^{(t)}, d_x)$$

and the update rules for the parameters  $n_{xk}$ ,  $a_k$  and  $b_k$  can be derived (for details see Appendix B)

$$n_{xk}^{(t)} = \frac{1}{z_x} W_{xk} \exp(\psi_0(a_k^{(t)}) - \log b_k)$$

$$a_k^{(t)} = \sum_{x=1}^N n_{xk}^{(t)} d_{xt} + \alpha_k \quad (2.7)$$

$$b_k = 1 + \beta_k$$

where  $z_x$  is the normalisation constant  $z_x = \sum_k n_{xk}$ .  $\psi_0$  is digamma function (logarithmic derivation of the gamma function).

Maximising the lower bound Eq.(2.6) with respect to  $w_{xk}$  gives

$$w_{xk} = \frac{\sum_t n_{xk}^{(t)} d_{xt}}{\lambda_k} \quad (2.8)$$

where  $\lambda_k = \sum_x w_{xk}$  is the normalisation constant.

The variational lower bound on the log-likelihood Eq.(2.6) then becomes

$$\mathcal{L} = \sum_t \left\{ \sum_k \mathbb{E}_H [\log h_{kt}] (\alpha_k - a_k^{(t)}) + \sum_k \log \frac{\Gamma(a_k^{(t)}) \beta_k^{\alpha_k}}{\Gamma(\alpha_k) b_k^{a_k^{(t)}}} + \sum_x d_{xt} \log z_x - \log \prod_x d_{xt}! \right\} \quad (2.9)$$

The algorithm is summarised in Algorithm 1 and has been implemented in MATLAB.

---

**Algorithm 1** Variational approximation updates.

---

Repeat until convergence:

1. For each time slice  $t$  of the stack: update  $n_{xk}^{(t)}$  and  $a_k^{(t)}$  according to Eq.(2.7). (Variational E step)
  2. Update  $W$  according to the Eq.(2.8). (Variational M step.)
  3. Compute the variational lower bound Eq.(2.9) and check for convergence.
- 

GaP model treats the intensities  $h_{kt}$  as hidden variables. The variational lower bound Eq.(2.6) bounds the approximation of the data likelihood Eq.(2.5) with hidden variables  $h_{kt}$  integrated out. It therefore naturally penalises the complexity of the model (Occam's razor [MacKay, 2003]) and can then be used for estimation of the  $K$ .

## 2.3 Analysis of the residuals

Different approach to the number of components  $K$  estimation is to analyse the  $N \times T$  residual matrix  $\mathbf{S}$  (entries  $s_{xt}$ ). After optimising the parameters of the model Eq.(1.1) for different values of  $K$ , we compute a normalised residual matrix

$$s_{xt} = \frac{d_{xt} - \sum_{k=1}^K w_{xk} h_{kt}}{\sqrt{\sum_{k=1}^K w_{xk} h_{kt}}}$$

Then the  $N \times N$  correlation matrix

$$\mathbf{C}_S = \mathbf{S}\mathbf{S}^T$$

and the  $N \times N$  matrix of the correlation coefficients  $\mathbf{R}_S$  with entries

$$r_{ij} = \frac{c_{ij}}{\sqrt{c_{ii}c_{jj}}} \quad (2.10)$$

Underestimation of the number of sources ( $K$  too small) will lead to correlations between some pixels as the model will try to explain multiple sources by one object. By increasing  $K$  the correlations should be expected to decrease until we reach a sufficient number of sources to explain the data and the residuals become uncorrelated.

## 2.4 Results

In the following section simulated data of 10 sources randomly spatially distributed are shown. Evaluation of the model with a classic NMF algorithm and the variational approximation is presented.  $K$  was varied in the range  $K = \{4, 5, 6 \dots 17\}$ .

Parameter	Value	Description
$T$	$10^3$	Number of time slices in the sequence
$K_{true}$	10	Number of sources in the simulated data
$b$	$10^2$ photons	Uniform background added to each time slice
$I_{max}$	$1.5 \cdot 10^3$ photons	Maximum intensity of a single source in one time slice
$\lambda_{em}$	655 nm	Emission wavelength
$NA$	1.2	Numerical aperture of the objective
pixel-size	106 nm	Size of a pixel in the sample plane
$\delta$	333 nm (3.1 pixels)	Radius of the region containing the sources ( $\delta = 0.61 \frac{\lambda_{em}}{NA}$ )

**Table 2.1:** Parameters of the simulation

Data were simulated according to the model Eq.(1.1) with parameter set to the values shown in Table 2.1:

1.  $K_{true} = 10$  spatial coordinates  $[x_k, y_k]$  confined to a circular region of with a radius  $\delta$  were generated ( $x$  and  $y$  coordinates generated from a uniform distribution subject to a spatial constraint to the circular area).  $\delta$  was equal to the Rayleigh's resolution limit ( $\delta = 0.61 \frac{\lambda_{em}}{NA}$ ).
2. In focus PSF was centred at each coordinate  $[x_k, y_k]$  ( $W$  in Eq.(1.1)).
3. Intensities of the individual sources over time  $h_{kt}$  were generated from a uniform distribution over an interval  $[0, \dots I_{max}]$  where  $I_{max}$  is the maximum intensity of the sources.
4. A homogeneous background of  $b$  was added to each frame of the time sequence.
5. Intensity in each pixel was corrupted with Poisson noise.

Data with lower density of the sources were simulated in the same way. However, the relative distances between the locations  $[x_k, y_k]$  of the individual sources (generated in step 1) were enlarged  $1.5\times$  and  $2.5\times$ . This way the geometrical configuration of the sources remains unchanged for all data sets. The locations of the sources are shown as blue circles in Fig. 2.1. A circle with a radius  $\delta$  is shown in green. The mean intensity image ( $\frac{1}{T} \sum_t d_{xt}$  - time sequence of QDs averaged over time) is shown in as grey scale image.

Principal component analysis (PCA) for the simulated data is shown in Fig. 2.2a-c. The first 20 PC eigenvalues are plotted. For the the dataset  $2.5\delta$  (Fig. 2.2a) we observe a distinct 'kink'



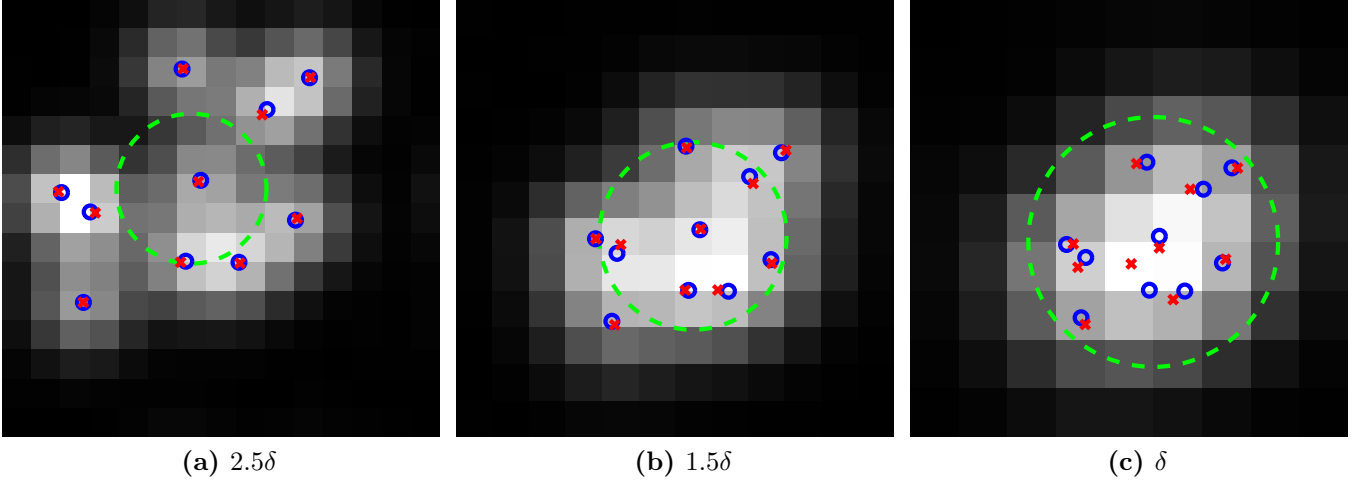


**Figure 2.1:** Simulated data (10 sources) with different densities. Sources in all three figures have the same geometrical configuration but different relative distances between the centres. All the sources are contained in a circular area with a radius  $2.5\delta$  (2.1a),  $1.5\delta$  (2.1b) and  $\delta$  (2.1c). Mean intensity over time is shown as a grey scale image. The true positions of the sources are shown as blue circles, estimated positions as red crosses. The green circle indicates an area with a radius  $\delta$ .

and for  $k > 10$  the PC values are negligible. For this dataset we can easily estimate  $K$ . However when the density of the sources becomes higher the ‘kink’ is much less pronounced (Fig. 2.2b-c) and the estimation of  $K$  from the PCA analysis becomes impossible.

We used the standard NMF updates [Lee and Seung, 2001]

$$\begin{aligned}
 w_{xk} &= \frac{w_{xk}}{\sum_{t=1}^T h_{kt}} [(D./WH)H^\top]_{xk} \\
 h_{kt} &= \frac{h_{kt}}{\sum_{x=1}^N w_{xk}} [W^\top(D./WH)]_{kt}
 \end{aligned} \tag{2.11}$$

to estimate the non-negative matrices  $W$  (images of the individual sources) and  $H$  (their intensities) of the model Eq.(1.1). The ‘./’ operation refers to an element-wise division. Different values of  $K = \{4, 5, \dots, 18\}$  were used and the log-likelihood

$$\log p(D|WH, K) = \sum_{x,t} \left\{ d_{xt} \log \sum_{k=1}^K w_{xk} h_{kt} - \sum_{k=1}^K w_{xk} h_{kt} - \log d_{xt}! \right\}$$

has been reported (Fig. 2.2d-f). We observe an increase of the likelihood function with increasing  $K$ . The estimated position of the separated sources ( $W$ ) with  $K = K_{true}$  is shown as blue circles in Fig. 2.1.

We analysed the correlation-coefficient matrix  $\mathbf{R}_S$  for the residuals Eq (2.10) and plotted the maximum entries in  $\mathbf{R}_S$  ( $\max_{ij}(r_{ij})$ ) in Fig. 2.2g-i. There is a significant drop in the correlation values for  $K = 10$  for the first two datasets. For the densest data Fig. 2.1c the correlations drop at about  $K = 8$  (Fig. 2.2i).

In Fig. 2.2j-l there is shown the variational lower bound  $\mathcal{L}(K)$  computed for the GaP with different values of  $K$  (section 2.2). For the easy (sparse) data set Fig. 2.1a  $\mathcal{L}(K)$  peaks for  $K = K_{true}$  (Fig. 2.2j) however, for the more dense data  $\mathcal{L}(K)$  reaches the maximum for  $K < K_{true}$ . This suggest that there is not enough evidence in the data for  $K = K_{true}$  as the data can be sufficiently explained with less complicated model  $K < K_{true}$ . It is probably worth emphasising that GaP model does not make any assumption about the time structure of the hidden variables  $h_{kt}$ . This information can provide a crucial evidence for the correct estimation of  $K$ .

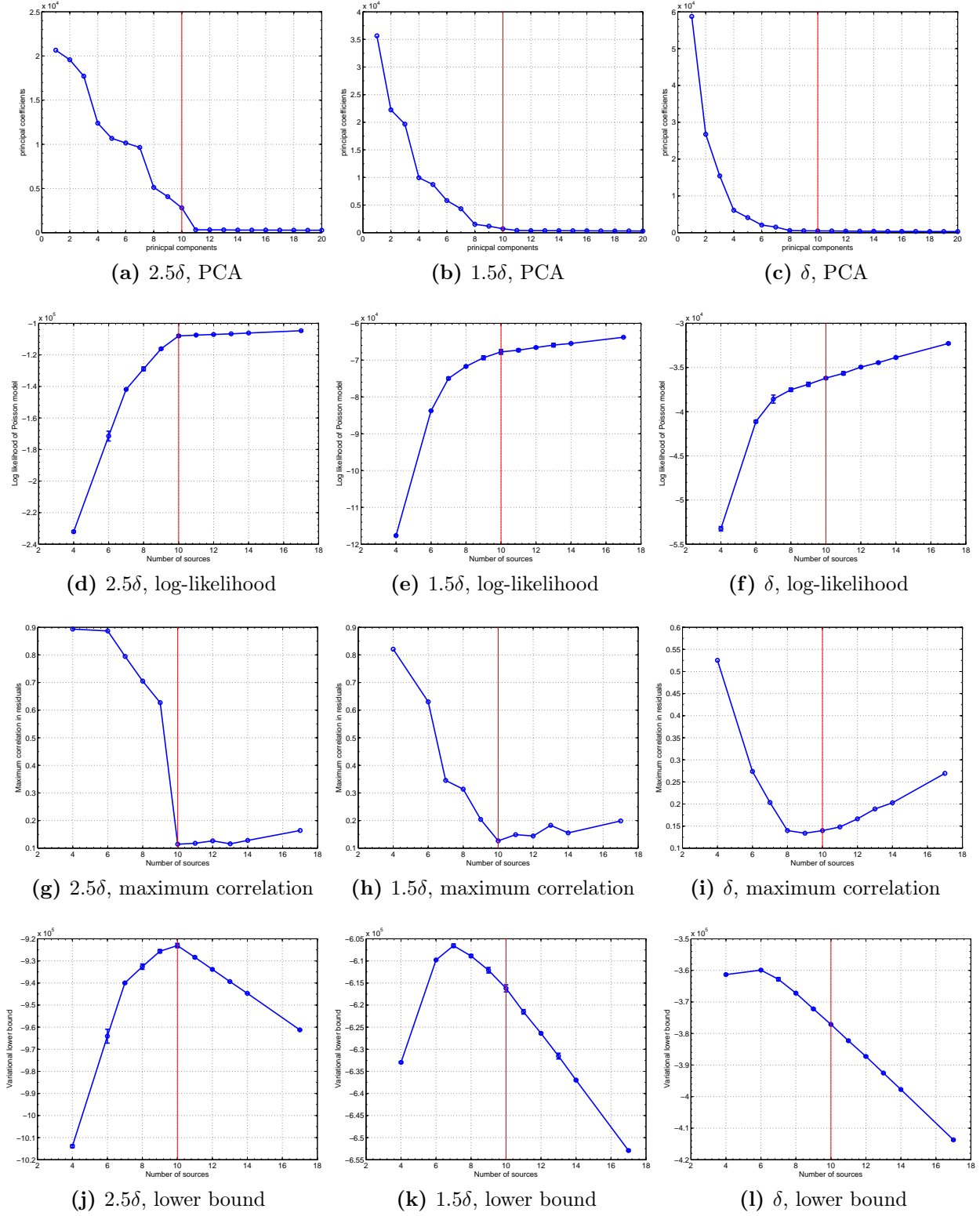


**Figure 2.2:** Number of components  $K$  estimation for sources contained in the circular area with radius  $2.5\delta$  (left column),  $1.5\delta$  (middle column) and  $\delta$  (right column) as shown in Fig. 2.1. The true value  $K_{true} = 10$  is indicated with a red vertical line.

From the results presented above it seems that the analysis of the residual correlations gives the most precise  $K$  estimation for high densities of sources. In order to investigate what is the ‘resolution’ of this  $K$  estimation we simulated datasets consisting of  $K_{true} = 2$  and  $K_{true} = 5$ . The sources were distributed uniformly on a circle with diameter  $d$ . Each data set was simulated 10 times as a different draws from a Poisson distribution (with identical parameters). Each dataset was evaluated with NMF for  $K = \{K_{true} - 1, K_{true}, K_{true} + 1\}$ . The maximum correlations coefficients in residuals  $\max_{ij}(r_{ij})$  has been recorded. The mean (and standard deviation) and the minimum values over 10 evaluation of the datasets for simulations with different  $d$  are shown in Fig. 2.3. The maximum residual correlations of the true model (the one used for the generation of the data) are plotted as a baseline for comparison.

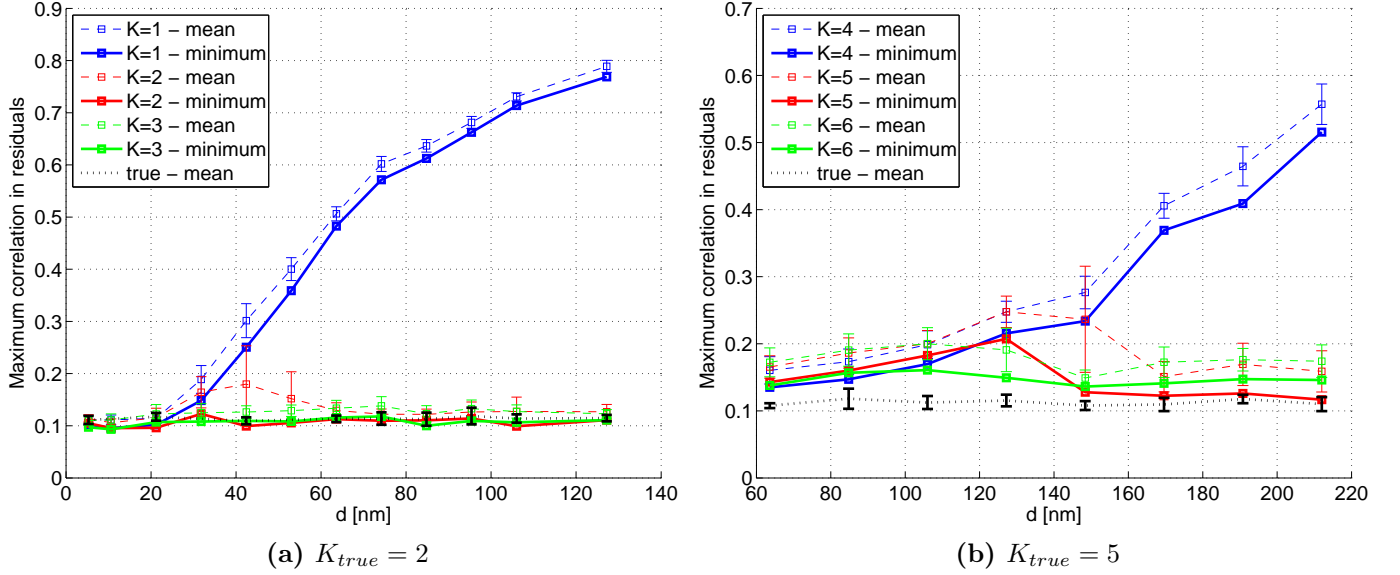


**Figure 2.3:** Maximum residual correlations. The mean (and standard deviation) and the minimum values of 10 evaluations of the datasets are shown. The maximum residual correlations of the true model (the one used for the generation of the data) are shown as black dotted line.

The correlations in residuals are much higher when  $K < K_{true}$ . Once  $K = K_{true}$  the correlations drop significantly to a baseline level. Further increase  $K > K_{true}$  does not result in lower correlations. This can be observed only if the distance  $d$  exceeds a certain ‘resolution’ limit  $d_l$ . From the Fig. 2.3 we can estimate  $d_l \approx 40$  nm ( $\lambda_{em}/16$ ) for two sources and  $d_l \approx 150$  nm for five sources.

### 3 Theoretical limits of the LM

Results from the variational approximation naturally bring a question about actual limits of the LM method. How close the sources can be in order to be possible to resolve them with the LM method? What are the limiting factors? Does the fluorescence intermittency (blinking) allow for higher resolution? We tried to address these question by examining the Cramér–Rao lower bound for the variance of the estimator on distance between two sources.

#### 3.1 Cramer Rao bound

If  $\mathcal{L}(\theta) = \log p(x|\theta)$  is a log-likelihood fucniton for data  $X$ , then a covariance matrix  $\mathbf{Q}$  of an unbiased estimator of  $\hat{\theta}$  is bounded by [Rao, 1945, Cover and Thomas, 1991]

$$\mathbf{Q} \geq \mathbf{I}^{-1}(\theta) \quad (3.1)$$

where  $\mathbf{I}(\theta)$  is the Fisher information matrix

$$I_{ij}(\theta) = -\mathbb{E} \left[ \frac{\partial^2 \mathcal{L}}{\partial \theta_i \partial \theta_j} \right] = \mathbb{E} \left[ \frac{\partial \mathcal{L}}{\partial \theta_i} \frac{\partial \mathcal{L}}{\partial \theta_j} \right] \quad (3.2)$$

The inequality Eq.(3.1) is in the sense that  $\mathbf{Q} - \mathbf{I}^{-1}(\theta)$  is a non-negative definite matrix.

#### 3.2 Fundamental resolution measure (FREM)

For PALM/STORM (section 1.2) the spatial resolution limit is determined by the localisation precision for an individual source. Cramér–Rao bound lower for the position estimation of a single source detected by a CCD camera is derived in [Ram et al., 2006b, Ram et al., 2006a]. The variance is shown to be proportional to  $1/\Lambda$  where  $\Lambda$  is the intensity of the source.

A fundamental resolution measure (FREM) for two sources separated by a distance  $d$  is shown as an alternative to the Rayleigh’s resolution criterion considering the photon statistic on the detector (CCD camera). The Fisher information is derived

$$I(d) = \frac{1}{4} \sum_{n=1}^N \frac{\left( \Lambda_1 \int_{C_n} \partial_x q(x - \frac{d}{2}) dx - \Lambda_2 \int_{C_n} \partial_x q(x + \frac{d}{2}) dx \right)^2}{\Lambda_1 \int_{C_n} q(x - \frac{d}{2}) dx + \Lambda_2 \int_{C_n} q(x + \frac{d}{2}) dx} \quad (3.3)$$

where  $\Lambda_i$  is the intensity of the  $i$ th source,  $q(x)$  is a response function of a source and  $C_n$  is an area of the  $n$ th pixel. The variance of the estimator on  $d$  is then

$$\text{var}(d) = I^{-1}(d)$$

A short summary is shown in Appendix C. There are certain problems with this formula, though. The limit  $d \rightarrow 0$  gives the Fisher information  $I(d) \rightarrow 0$  ( $\text{var}(d) \rightarrow \infty$ ) for situation when  $\Lambda_1 = \Lambda_2$ . However, the variance remains finite ( $I(d) \neq 0$ ) when  $\Lambda_1 \neq \Lambda_2$  (see discussion in Appendix C). The formula also gives  $I(d) \neq 0$  even for the situation when one of the sources is not present ( $\Lambda_i = 0$ ). This stems from the fact that the response function of the sources are assumed to be located at  $\pm \frac{d}{2}$  which implicitly assumes the knowledge of the origin location. Only one source is then needed to determined the distance  $\frac{d}{2}$ .

#### 3.3 An alternative derivation of the FREM

We derived an alternative FREM formula for two sources situation (details in Appendix C). We assume two sources located at positions  $c_1$  and  $c_2$ . The response functions (we assume here the

identical PSF  $q(x)$  for both sources) are  $f_1 = q(x - c_1)$  and  $f_2 = q(x - c_2)$ . The distance between the two sources is  $d = c_1 - c_2$  and the variance of  $d$  is given by

$$\text{var}(d) = Q_{11} + Q_{22} - 2Q_{12}$$

where  $\mathbf{Q}$  is a covariance matrix  $\mathbf{Q} = \mathbf{I}^{-1}(\theta)$  and  $\mathbf{I}(\theta)$  is a (symmetric) Fisher information matrix Eq.(3.2).

For a Poisson distributed pixel counts (this assumes that data are corrupted with Poisson noise only)

$$p(n_p|\theta_p) = \text{Po}(n_p; \lambda_p)$$

where  $\lambda_p$  is the mean value of the  $p$ th pixel:

$$\lambda_p = \int_{C_p} \lambda dx = \int_{C_p} \Lambda_1 f_1(x) + \Lambda_2 f_2(x) dx \quad (3.4)$$

The log-likelihood function for  $N$  pixels

$$\log p(n|\theta) = \sum_{p=1}^N p(n_p|\lambda_p) \quad (3.5)$$

and the Fisher information matrix becomes (Appendix C)

$$I_{ij}(\theta) = \sum_{p=1}^N \frac{1}{\lambda_p} \frac{\partial \lambda_p}{\partial \theta_i} \frac{\partial \lambda_p}{\partial \theta_j}$$

The covariance matrix  $\mathbf{Q}$  is then

$$\mathbf{Q} = \mathbf{I}^{-1}(\theta) = \frac{1}{I_{11}I_{12} - I_{12}^2} \begin{pmatrix} I_{22} & -I_{12} \\ -I_{12} & I_{11} \end{pmatrix}$$

and the variance of  $d = c_1 - c_2$

$$\text{var}(d) = (1, -1)^T \cdot \mathbf{Q} \cdot (1, -1) = \frac{I_{11} + I_{22} + 2I_{12}}{I_{11}I_{12} - I_{12}^2} \quad (3.6)$$

For a symmetrical PSF  $q(x - d) = q(x + d)$  we showed (Appendix C) the entries of the Fisher information matrix

$$\begin{aligned} I_{ii} &= \sum_{n=1}^N \frac{(\Lambda_i q'_n)^2}{\Lambda_i q_n + \Lambda_j q_n(d)} \\ I_{ij} &= \sum_{n=1}^N \frac{\Lambda_i \Lambda_j q'_n(0) q'_n(d)}{\Lambda_i q_n + \Lambda_j q_n(d)} \text{ for } i \neq j \end{aligned} \quad (3.7)$$

where  $q_n(d) = \int_{C_n} q(x - d) dx$  ( $q_n(0) = q_n$ ) and  $q'_n(d) = \int_{C_n} \frac{\partial q(x-d)}{\partial x} dx$  ( $q'_n(0) = q'_n$ ).

As shown in Appendix C variance defined in Eq.(3.6) have very reasonable behaviour in the limits: the limit  $d \rightarrow 0$  gives  $\text{var}(d) \rightarrow \infty$  for any value  $\Lambda_i, \Lambda_j$ . The variance is also infinite if one of the sources is zero  $\Lambda_i = 0$  as it does not make any assumption about the symmetry with respect to the origin ( $d = c_1 - c_2$ ).

For sources well separated  $d \rightarrow \infty$  the off-diagonal elements of the Fisher information matrix vanish ( $I_{ij} = 0$  for  $i \neq j$ ) and the variance becomes  $\text{var}(d) = \text{var}(c_1) + \text{var}(c_2)$  (sum of the variances for localisation of individual sources).

### 3.4 FREM for blinking sources

One of the fundamental questions is whether the fluorescence intermittency (QD blinking) allows for higher resolution compared to the situation when the sources remains static over time. To address this question we assume a simple model of Poisson distributed data with mean values  $\lambda_n$  shown in Eq.3.4. We assume the intensity vector of the two sources  $\mathbf{\Lambda} = (\Lambda_1, \Lambda_2)$  to be a random variable distributed over four distinctive states

$$\{\mathbf{\Lambda}^1 = (\Lambda_1, 0), \mathbf{\Lambda}^2 = (0, \Lambda_2), \mathbf{\Lambda}^3 = (\Lambda_1, \Lambda_2), \mathbf{\Lambda}^4 = (0, 0)\}$$

This simulates a simple blinking model of two QDs. If the state of  $\mathbf{\Lambda}$  were known we would write the likelihood function as

$$l(\theta) = p(n, \mathbf{\Lambda}|\theta) = \prod_{p=1}^N \prod_{i=1}^4 p(n_p|\theta, \mathbf{\Lambda}^i) p(\mathbf{\Lambda}^i)$$

and the Fisher information matrix would become (Appendix C)

$$I(\theta) = \sum_{i=1}^4 p(\mathbf{\Lambda}^i) \sum_{p=1}^N \frac{1}{\lambda_p(\theta, \mathbf{\Lambda}^i)} \left( \frac{\partial \lambda_p(\theta, \mathbf{\Lambda}^i)}{\partial \theta} \right)^2 \quad (3.8)$$

which is the expectation value (with respect to the states  $\mathbf{\Lambda}$ ) of the Fisher information matrix Eq.(3.7).

However, we assume that the variable  $\mathbf{\Lambda}$  is fully described by the probability  $p(\mathbf{\Lambda})$  over the states. The exact state in each situation is unknown. Therefore we have to integrate over  $\mathbf{\Lambda}$  and the likelihood function is then

$$l(\theta) = \prod_{p=1}^N p(n_p|\theta) = \prod_{p=1}^N \sum_{i=1}^4 p(n_p, \mathbf{\Lambda}^i|\theta) = \prod_{p=1}^N \sum_{i=1}^4 p(n_p|\theta, \mathbf{\Lambda}^i) p(\mathbf{\Lambda}^i) \quad (3.9)$$

This complicates the evaluation of the Fisher information matrix Eq.(3.2) because of the summation within the logarithm in the log-likelihood

$$\mathcal{L}(\theta) = \log l(\theta) = \sum_p \log \sum_{i=1}^4 p(n_p|\theta, \mathbf{\Lambda}^i) p(\mathbf{\Lambda}^i)$$

In Appendix C we show that the Fisher information matrix for  $p(\mathbf{\Lambda}^i) = \frac{1}{4}$  for all  $i$

$$I_{rs}(\theta) = \sum_{p=1}^N \mathbb{E}_p \left[ \frac{\left( \sum_{i=1}^4 \frac{\partial \text{Po}(\lambda_p^i)}{\partial c_r} \right) \left( \sum_{l=1}^4 \frac{\partial \text{Po}(\lambda_p^l)}{\partial c_s} \right)}{\left( \sum_{j=1}^4 \text{Po}(\lambda_p^j) \right)^2} \right] \quad (3.10)$$

where  $\lambda_p^i = \lambda_p(\mathbf{\Lambda}^i)$  is the mean intensity in the  $p$ th pixel when  $\mathbf{\Lambda}$  is in the state  $\mathbf{\Lambda}^i$ .  $\mathbb{E}_p[\cdot]$  represents the expectation value with respect to  $p(n_p|\theta)$  in Eq.(3.9). Expressing the derivatives and the expectation value gives

$$I_{rs}(\theta) = \frac{1}{2} \sum_{p=1}^N \left( \frac{\partial \lambda_p^r}{\partial c_r} \right) \left( \frac{\partial \lambda_p^s}{\partial c_s} \right) \sum_{n_p \geq 0} \left[ \frac{\left( \sum_{i=\{r,3\}} \text{Po}(n_p; \lambda_p^i) \frac{(n_p - \lambda_p^i)}{\lambda_p^i} \right) \left( \sum_{l=\{s,3\}} \text{Po}(n_p; \lambda_p^l) \frac{(n_p - \lambda_p^l)}{\lambda_p^l} \right)}{\sum_{j=1}^4 \text{Po}(n_p; \lambda_p^j)} \right]$$

In Appendix C we show that the limit  $d \rightarrow 0$  gives  $\text{var}(d) \rightarrow \infty$  and the limit  $d \rightarrow \infty$  gives  $\text{var}(d) = \frac{1}{I_{11}} + \frac{1}{I_{22}} = 2 \left( \frac{1}{I_{11}^{\text{static}} - \epsilon} + \frac{1}{I_{22}^{\text{static}} - \epsilon} \right) > 2\text{var}(d^{\text{static}})$  where  $I^{\text{static}}$  and  $\text{var}^{\text{static}}(d)$  is the Fisher information matrix and the variance, respectively, of the static case (section 3.3). The factor 2 in the expression for the variance comes from the fact that the total number of photons in this model is the factor of two smaller then in the static case.

### 3.5 Simulations

We made a numerical computation of the  $\text{var}(d)$  for two sources with equal intensity  $\Lambda_1 = \Lambda_2 = \Lambda$ . The parameters of the simulated sources are shown in Tab. 2.1. We kept the total intensity (total photon count) equal for both static and the blinking case.

In the static case Eq.(3.6) the variance  $\text{var}(d) \propto \frac{1}{\Lambda}$  as each entry of the Fisher information matrix  $I_{pq} \propto \Lambda$  (Eq.(3.7)). The intensity of the sources  $\Lambda$  is only a linear scaling factor. In the blinking case Eq.(3.10) the dependency on  $\Lambda$  is complicated as the expectation in Eq.(3.10) cannot be easily evaluated. The results for different values of  $\Lambda$  are shown in Fig. 3.1.

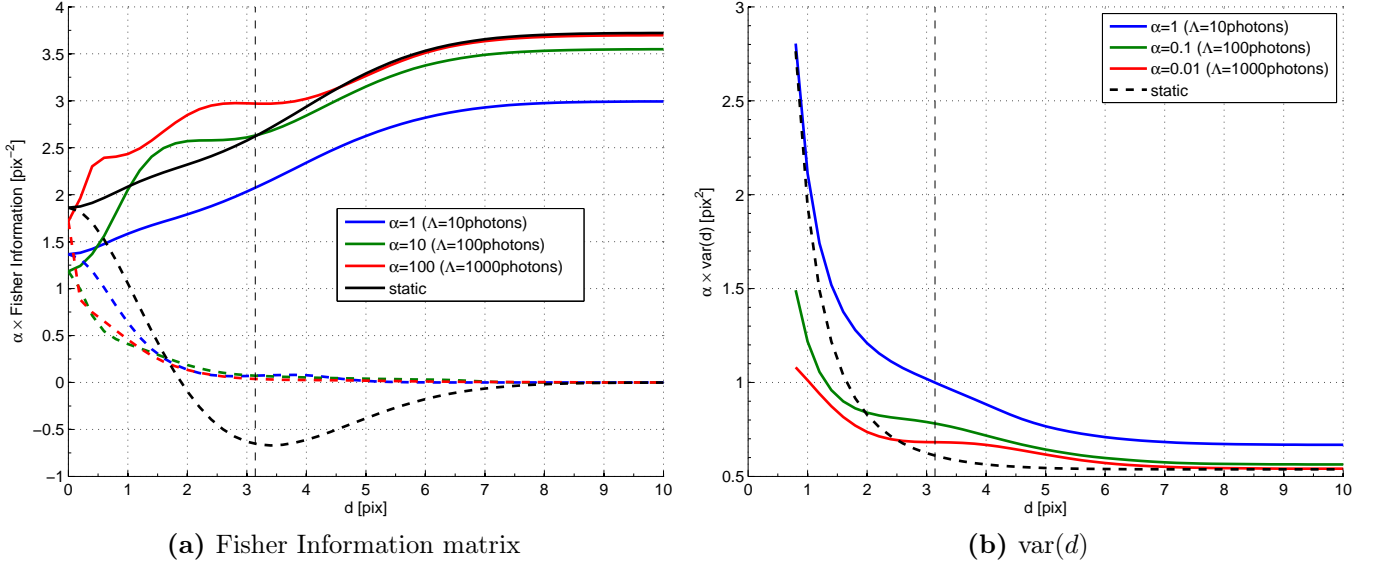


**Figure 3.1:** Left: Fisher information matrix entries. Solid lined show diagonal entries, broken line show the off-diagonal elements. Right: variance of the distance estimation. Black lines show the results for the static case Eq.(3.7). Colour lines show the blinking situation Eq.(3.10) for different intensities  $\Lambda$  of the sources. The values must be scaled by a factor  $\alpha$  shown in the legend. The vertical broken line indicates the Rayleigh resolution limit.

### 3.6 Conclusions

The alternative derivation of the FREM provides correction to the formula published in [Ram et al., 2006b]. Results presented in the Fig. 3.1 suggest that the intensity blinking of the sources can increase the localisation precision for the situations when the sources are very close. However, for well separated sources ( $d \rightarrow \infty$  limit) the static situation provide upper bound for the entries of the Fisher information matrix of blinking model (Eq.(C.11)). In this configuration the static situation allows for more precise localisation. The intersection points of the curves for static and blinking model depends on the intensity of the sources (Fig. 3.1b).

The results here, however, are computed for the model with no background. More investigation will be needed to explore the effect of the background.

## 4 Out of focus PSF

The point spread function (PSF) is a rather complicated 3D object. A scan along the axial direction through a PSF of an optical microscope (Fig. 4.1) shows the characteristic ringings for out-of-focus PSF. In a real biological sample PSF from different focal planes can overlap. As the NMF does not make any assumption about the PSFs of the individual sources (parameter matrix  $W$ ), it is possible to separate overlapping QDs located in different axial positions. This can be possible used for the 3D localisation of the sources. Moreover the PSF of the individual sources can differ due to the aberrations caused by imperfections of the microscope or by inhomogenities of the refractive index in the sample. However, the PSF of each source must remain constant during the data acquisition.

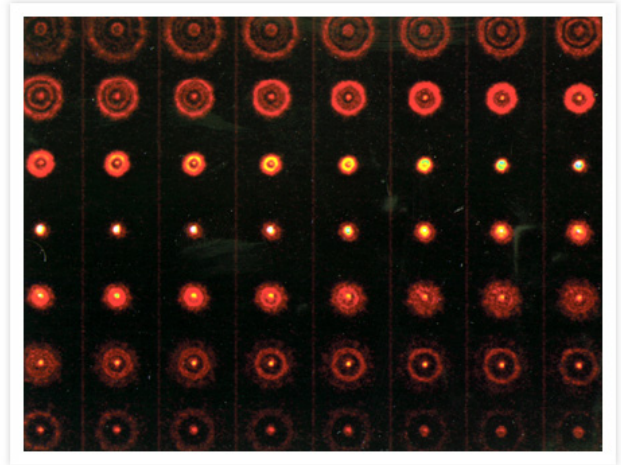


**Figure 4.1:** Point spread function for different focal planes. [www.invitrogen.com](http://www.invitrogen.com)

### 4.1 Results

We recorded a sample of the QDs deposited on a cover slip. Slight variations in the focal plane occurs between the individual QDs which results in different PSFs for each source.

We acquired  $10^3$  images with 100 ms exposure time (the total acquisition time is about 2 mins). Several images from the time stack are shown in Fig. 4.2. The PCA coefficients of the data are shown in Fig. 4.3a.

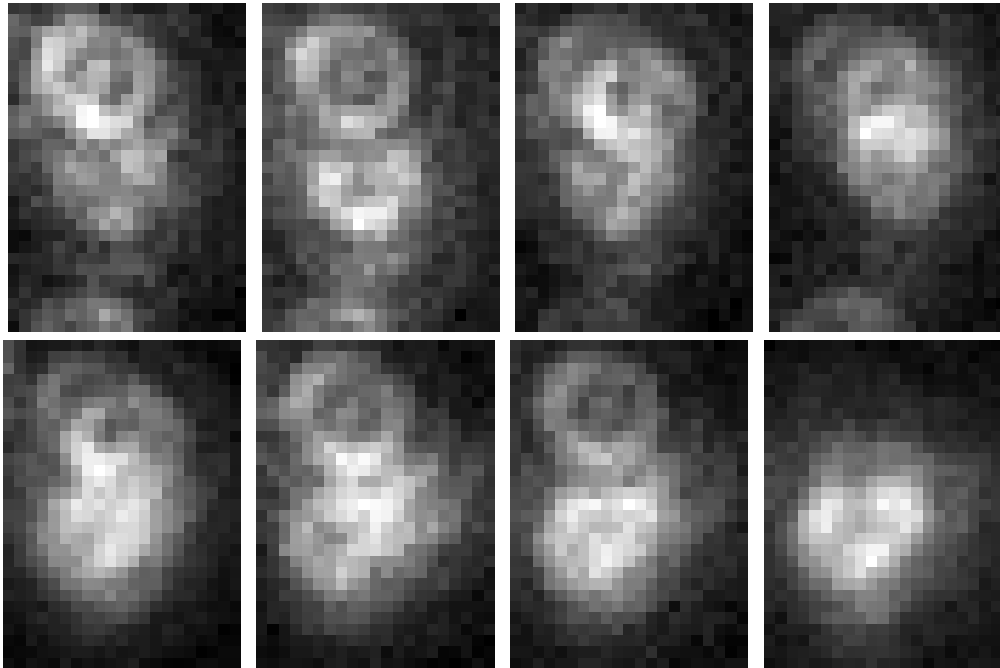


**Figure 4.2:** Eight images (out of  $10^3$ ) of the blinking QD time series.

We used the standard NMF algorithm [Lee and Seung, 2001] with different number of sources  $K = \{7, 8 \dots 19\}$  and computed the maximum correlation coefficient of the residuals Eq.(2.10).



The results are shown in Fig. 4.3b. Unlike the PCA (Fig. 4.3a) we can observe a ‘kink’ for  $K = 13$ . Increasing  $K$  does not lead to a further decrease of the correlations in residuals. Separated individual PSF ( $W$ ) for  $K = 13$  are shown in Fig. 4.4b. The separated individual PSFs correspond to QDs at different axial positions (see Fig. 4.1).

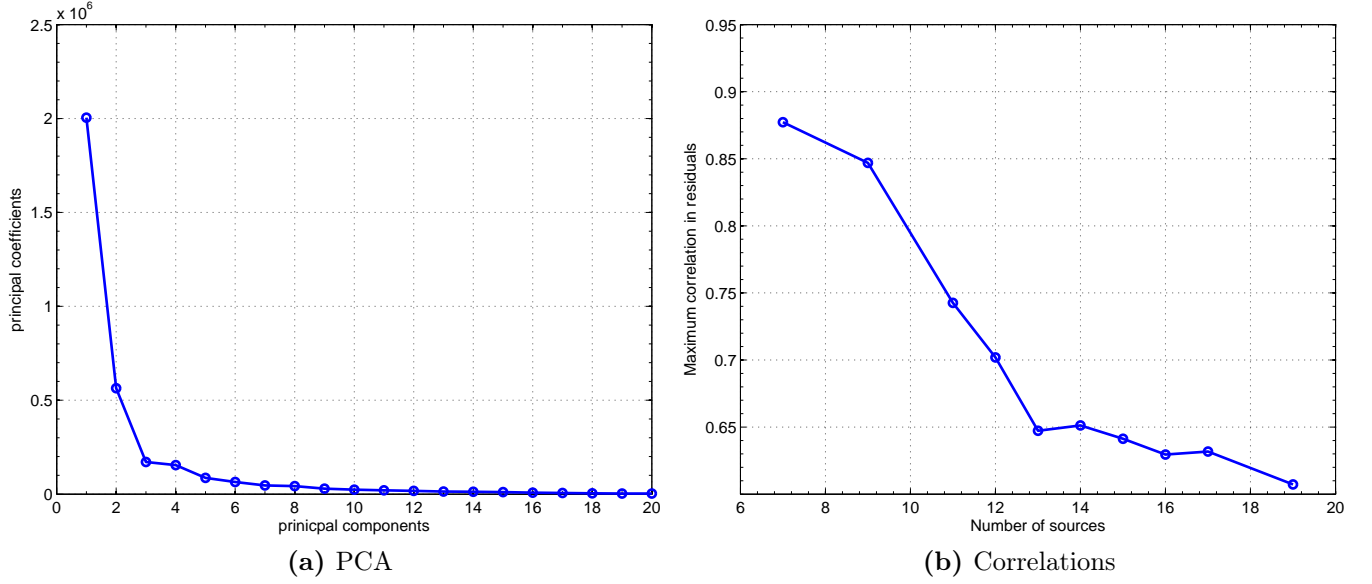


**Figure 4.3:** Estimation of  $K$

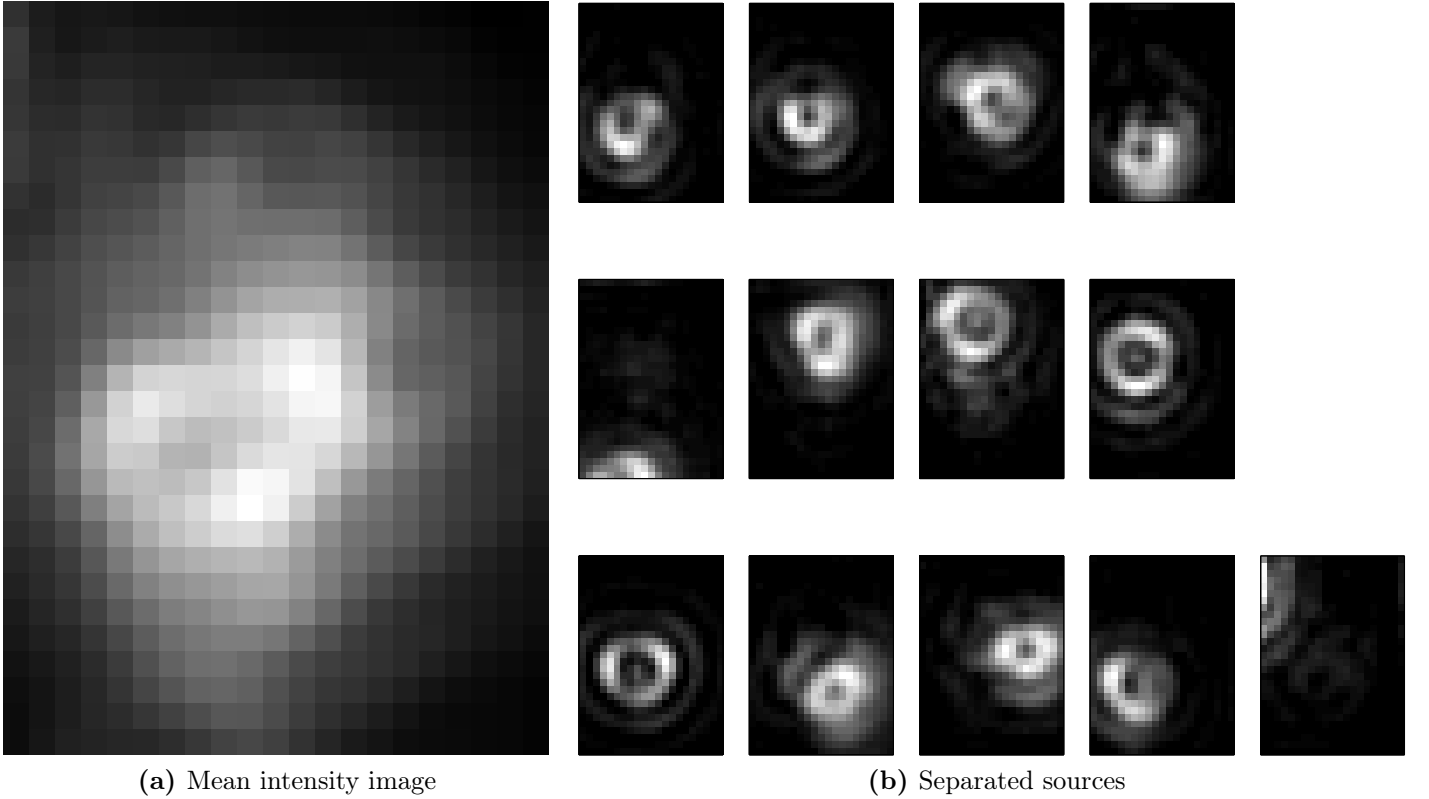


**Figure 4.4:** Left: mean intensity image correspond to a standard wide-field image. Right: separated individual sources for  $K = 13$ .

## 5 Conclusion and Future work

We demonstrated the capability of NMF to separate individual highly overlapping sources with different PSFs (Fig. 4.4b). The estimation of  $K$  (number of sources in data) remains a difficult task for realistic data sets. The variational lower bound (section 2.2) provides correct estimates only for relatively easy data (Fig. 2.1a).  $K$  is severely underestimated for the data with higher densities of the sources (Fig. 2.2). The most accurate estimation of  $K$  were achieved by analysis of the correlations in the residuals (Fig. 2.2). The ‘resolution’ of this method for two and five sources is shown in Fig. 2.3. The use of information about the time structure of the data would certainly help in this task.

Blinking behaviour of the sources has been theoretically demonstrated to allow for higher localisation precision (Fig. 3.1b) especially for brighter sources. Further analysis is required to examine the effect of the background in the data to provide more realistic description of the resolution limit.

### 5.1 Time series

comments on [Molgedey and Schuster, 1994] ?

### 5.2 Future work and direction of the project

# References

- [Baddeley et al., 2009] Baddeley, D., Jayasinghe, I. D., Cremer, C., Cannell, M. B., and Soeller, C. (2009). Light-induced dark states of organic fluochromes enable 30 nm resolution imaging in standard media. *Biophysical journal*, 96(2):L22–4.
- [Bates et al., 2007] Bates, M., Huang, B., Dempsey, G. T., and Zhuang, X. (2007). Multicolor super-resolution imaging with photo-switchable fluorescent probes. *Science (New York, N.Y.)*, 317(5845):1749–53.
- [Bishop, 2006] Bishop, C. M. (2006). *Pattern Recognition and Machine Learning*. Springer.
- [Blei et al., 2003] Blei, D. M., Ng, A. Y., and Jordan, M. I. (2003). Latent Dirichlet Allocation. *Journal of Machine Learning Research*, 3(4-5):993–1022.
- [Born et al., 1975] Born, M., Wolf, E., and Bhatia, A. B. (1975). *Principles of optics*, volume 10. Pergamon Pr.
- [Buntine and Jakulin, 2006] Buntine, W. and Jakulin, A. (2006). Discrete component analysis. In Saunders, C., Grobelnik, M., Gunn, S., and Shawe-Taylor, J., editors, *Subspace, Latent Structure and Feature Selection*, pages 1–33. Springer.
- [Canny, 2004] Canny, J. (2004). GaP: a factor model for discrete data. In *Proceedings of the 27th annual international ACM SIGIR conference on Research and development in information retrieval*, pages 122–129. ACM.
- [Cover and Thomas, 1991] Cover, T. M. and Thomas, J. A. (1991). *Elements of Information Theory*, volume 1 of *Wiley Series in Telecommunications*. Wiley.
- [Fish et al., 1995] Fish, D. A., Brinicombe, A. M., Pike, E. R., and Walker, J. G. (1995). Blind deconvolution by means of the Richardson–Lucy algorithm. *J. Opt. Soc. Am. A*, 12(1):58–65.
- [Gordon et al., 2004] Gordon, M., Ha, T., and Selvin, P. (2004). Single-molecule high-resolution imaging with photobleaching. *Proceedings of the National Academy of Sciences of the United States of America*, 101(17):6462.
- [Harrington et al., 2008] Harrington, P., Anderson, J., Rieger, B., Lidke, D., and Lidke, K. A. (2008). Poster: A Bayesian Approach to Fluorescence Intermittency Based Localization Microscopy. *Supplement of Biophysical Journal*, 96:20–20.
- [Hess et al., 2006] Hess, S. T., Girirajan, T. P. K., and Mason, M. D. (2006). Ultra-high resolution imaging by fluorescence photoactivation localization microscopy. *Biophysical journal*, 91(11):4258–72.
- [Holmes, 1992] Holmes, T. J. (1992). Blind deconvolution of quantum-limited incoherent imagery: maximum-likelihood approach: errata. *J. Opt. Soc. Am. A*, 9(11):2097.
- [Huang et al., 2008] Huang, B., Wang, W., Bates, M., and Zhuang, X. (2008). Three-dimensional super-resolution imaging by stochastic optical reconstruction microscopy. *Science (New York, N.Y.)*, 319(5864):810–3.
- [Hyvärinen and Oja, 2000] Hyvärinen, a. and Oja, E. (2000). Independent component analysis: algorithms and applications. *Neural networks : the official journal of the International Neural Network Society*, 13(4-5):411–30.

- [Jaiswal and Simon, 2004] Jaiswal, J. K. and Simon, S. M. (2004). Potentials and pitfalls of fluorescent quantum dots for biological imaging. *Trends in cell biology*, 14(9):497–504.
- [Joshi and Miller, 1993] Joshi, S. and Miller, M. I. (1993). Maximum  $\alpha$  posteriori estimation with Good’s roughness for three-dimensional optical-sectioning microscopy. *J. Opt. Soc. Am. A*, 10(5):1078–1085.
- [Kuno et al., 2001] Kuno, M., Fromm, D. P., Hamann, H. F., Gallagher, A., and Nesbitt, D. J. (2001). "On"/"off" fluorescence intermittency of single semiconductor quantum dots. *The Journal of Chemical Physics*, 115(2):1028.
- [Lagerholm et al., 2006] Lagerholm, B. C., Averett, L., Weinreb, G. E., Jacobson, K., and Thompson, N. L. (2006). Analysis method for measuring submicroscopic distances with blinking quantum dots. *Biophysical journal*, 91(8):3050–60.
- [Lee and Seung, 2001] Lee, D. and Seung, H. (2001). Algorithms for non-negative matrix factorization. *Advances in neural information processing systems*, 13.
- [Lidke and Heintzmann, 2007] Lidke, K. and Heintzmann, R. (2007). Localization fluorescence microscopy using quantum dot blinking. In *Biomedical Imaging: From Nano to Macro, 2007. ISBI 2007. 4th IEEE International Symposium on*, pages 936–939. IEEE.
- [Lidke et al., 2005] Lidke, K. a., Rieger, B., Jovin, T. M., and Heintzmann, R. (2005). Superresolution by localization of quantum dots using blinking statistics. *Optics Express*, 13(18):7052.
- [Lucy, 1974] Lucy, L. B. (1974). An iterative technique for the rectification of observed distributions. *The Astronomical Journal*, 79:745.
- [MacKay, 2003] MacKay, D. J. C. (2003). *Information Theory, Inference, and Learning Algorithms*, volume 22. Cambridge University Press.
- [Michalet et al., 2005] Michalet, X., Pinaud, F. F., Bentolila, L. a., Tsay, J. M., Doose, S., Li, J. J., Sundaresan, G., Wu, a. M., Gambhir, S. S., and Weiss, S. (2005). Quantum dots for live cells, in vivo imaging, and diagnostics. *Science (New York, N.Y.)*, 307(5709):538–44.
- [Molgedey and Schuster, 1994] Molgedey, L. and Schuster, H. (1994). Separation of a mixture of independent signals using time delayed correlations. *Physical Review Letters*, 72(23):3634–3637.
- [Ober et al., 2004] Ober, R. J., Ram, S., and Ward, E. S. (2004). Localization accuracy in single-molecule microscopy. *Biophysical journal*, 86(2):1185–200.
- [Qu et al., 2004] Qu, X., Wu, D., Mets, L., and Scherer, N. (2004). Nanometer-localized multiple single-molecule fluorescence microscopy. *Proceedings of the National Academy of Sciences of the United States of America*, 101(31):11298.
- [Ram et al., 2006a] Ram, S., Sally Ward, E., and Ober, R. J. (2006a). A Stochastic Analysis of Performance Limits for Optical Microscopes. *Multidimensional Systems and Signal Processing*, 17(1):27–57.
- [Ram et al., 2006b] Ram, S., Ward, E. S., and Ober, R. J. (2006b). Beyond Rayleigh’s criterion: a resolution measure with application to single-molecule microscopy. *Proceedings of the National Academy of Sciences of the United States of America*, 103(12):4457–62.
- [Rao, 1945] Rao, C. R. (1945). Information and accuracy attainable in the estimation of statistical parameters. *Bull Calcutta Math Soc*, 37:81–91.

- [Rayleigh, 1896] Rayleigh, L. (1896). On the theory of optical images with special reference to the optical microscope. *Phil Mag*, 5(42):167–195.
- [Richardson, 1972] Richardson, W. H. (1972). Bayesian-Based Iterative Method of Image Restoration. *J. Opt. Soc. Am.*, 62(1):55–59.
- [Shroff et al., 2008] Shroff, H., Galbraith, C., Galbraith, J., and Betzig, E. (2008). Live-cell photoactivated localization microscopy of nanoscale adhesion dynamics. *Nature Methods*, 5(5):417–423.
- [Stefani et al., 2009] Stefani, F. D., Hoogenboom, J. P., and Barkai, E. (2009). Beyond quantum jumps: Blinking nanoscale light emitters. *Physics Today*, 62(2):34.
- [Thompson, 2002] Thompson, R. (2002). Precise Nanometer Localization Analysis for Individual Fluorescent Probes. *Biophysical Journal*, 82(5):2775–2783.
- [van Kempen et al., 1997] van Kempen, G. M. P., van Vliet, L. J., Verveer, P. J., and van der Voort, H. T. M. (1997). A quantitative comparison of image restoration methods for confocal microscopy. *Journal of Microscopy*, 185(3):354–365.
- [Verveer et al., 1999] Verveer, P. J., Gemkow, M. J., and Jovin, T. M. (1999). A comparison of image restoration approaches applied to three-dimensional confocal and wide-field fluorescence microscopy. *Journal of microscopy*, 193(1):50–61.
- [Zhang et al., 2007] Zhang, B., Zerubia, J., and Olivo-Marin, J. (2007). Gaussian approximations of fluorescence microscope point-spread function models. *Applied Optics*, 46(10):1819–1829.

## A NMF as a minimisation of Kullback–Leibler divergence

A generalised Kullback-Liebler (KL) divergence between two (un normalised) discrete variables  $P_i$  and  $Q_i$  is defined

$$KL(P \parallel Q) = \sum_i \left( Q_i \log \frac{Q_i}{P_i} - Q_i + P_i \right)$$

NMF algorithm [Lee and Seung, 2001] minimised the KL divergence between the data matrix  $D$  and the factorised model  $WH$  (Eq.(1.1))

$$\min_{W, H \geq 0} KL(D \parallel WH) = \min_{W, H \geq 0} - \sum_{xt} \left( d_{xt} \log \sum_{k=1}^K w_{xk} h_{kt} - \sum_{k=1}^K w_{xk} h_{kt} \right) + C \quad (\text{A.1})$$

where  $C$  is a constant independent on  $W$  and  $H$ .

Log-likelihood function of the model Eq.(1.1) under an assumption of Poisson noise

$$\log p(D|W, H) = \sum_{x,t} \log \left( \frac{d_{xt}^{\sum_k w_{xk} h_{kt}} e^{-\sum_k w_{xk} h_{kt}}}{d_{xt}!} \right) = \sum_{xt} \left( d_{xt} \log \sum_{k=1}^K w_{xk} h_{kt} - \sum_{k=1}^K w_{xk} h_{kt} \right) + D$$

where  $D$  is a constant independent on  $W$  and  $H$ . Comparison with Eq.(A.1) shows that minimisation of the KL divergence between data and the model is equivalent to the maximisation of the log-likelihood function of the model with assumption of the Poisson noise.

## B Variational approximation for GaP model

This is a derivation of the variational approximation of the GaP model [Buntine and Jakulin, 2006]. From the main text there is a different notation: data  $d \rightarrow w$ , hidden variables (intensities)  $h \rightarrow l$ , parameters of the model (PSFs of the individual sources)  $w \rightarrow \theta$ .

Gamma-Poisson (GP) model [Canny, 2004]:

$$\mathbb{E}_{w \sim p(w|l, \theta)} [w_j] = \sum_{k=1}^K \theta_{jk} l_k$$

- $w_j$  word count of  $j$ th word in a document

$$w_j \sim \text{Po}(w_j; (\theta \mathbf{l})_j) = \frac{(\theta \mathbf{l})_j^{w_j} \exp(-(\theta \mathbf{l})_j)}{w_j!}$$

- $l_k$  component scores (vector  $\mathbf{l}$ ) that indicate amount of the component in the document

$$l_k \sim \text{Gamma}(l_k; \alpha_k, \beta_k) = \frac{l_k^{\alpha_k-1} \beta_k^{\alpha_k} \exp(-\beta_k l_k)}{\Gamma(\alpha_k)}$$

- $\theta$  component loading matrix of size  $J \times K$ .  $\theta_{jk}$  controls partition of the  $k$ th component in the  $j$ th word

The log-likelihood of this model:

$$\log p(\mathbf{w}, \mathbf{l} | \theta, \text{GP}, K) = \sum_{k=1}^K \left\{ \alpha_k \log(\beta_k) + (\alpha_k - 1) \log l_k - \beta_k l_k - \log \Gamma(\alpha_k) + \sum_{j=1}^J [w_j \log(\theta \mathbf{l})_j - (\theta \mathbf{l})_j - \log w_j!] \right\} \quad (\text{B.1})$$

$$= \sum_{k=1}^K \log \text{likelihood of } l_k + \sum_{j=1}^J \log \text{likelihood of } w_j \text{ given } \mathbf{l}$$

## Components assignment for words.

Introducing a discrete latent vector  $\mathbf{c}$  whose total count is  $\sum_j w_j$ . The count  $c_k$  gives the count of words in the document appearing in the  $k$ th component. It is derived from a latent matrix  $\mathbf{V}$  of size  $J \times K$  (entries  $v_{jk}$ ).

$$\begin{aligned}\sum_{j=1}^J v_{jk} &= c_k \\ \sum_{k=1}^K v_{jk} &= w_j\end{aligned}$$

The distribution underlying the GP model now becomes

$$\begin{aligned}l_k &\sim \text{Gamma}(l_k; \alpha_k, \beta_k) \\ c_k &\sim \text{Po}(c_k; l_k) \\ v_{j,k} &\sim \text{Multinom}(v_{jk}; \theta_{jk}, c_k) = c_k! \prod_j \frac{\theta_{jk}^{v_{jk}}}{v_{jk}!}\end{aligned}$$

Proof:

We have  $p(c_k|l_k) = \text{Po}(c_k; l_k)$  and  $p(v_{jk}|c_k) = \text{Binom}(v_{jk}; \theta_{jk}, c_k) = \binom{c_k}{v_{jk}} \theta_{jk}^{v_{jk}} (1 - \theta_{jk})^{c_k - v_{jk}}$  (probability of having  $v_{jk}$  counts in  $c_k$  counts). Then:

$$\begin{aligned}p(v_{jk}|l_k) &= \sum_{c_k} p(v_{jk}|c_k) p(c_k|l_k) \\ &= \sum_{c_k=v_{jk}}^{\infty} \frac{c_k!}{v_{jk}!(c_k - v_{jk})!} \theta_{jk}^{v_{jk}} (1 - \theta_{jk})^{c_k - v_{jk}} \times \frac{l_k^{c_k} \exp(-l_k)}{c_k!} \\ &= \frac{\exp(-l_k) \theta_{jk}^{v_{jk}}}{v_{jk}!} \sum_{c_k=v_{jk}}^{\infty} \frac{l_k^{c_k} (1 - \theta_{jk})^{c_k - v_{jk}}}{(c_k - v_{jk})!} \quad | \alpha_{jk} = c_k - v_{jk} \\ &= \frac{\exp(-l_k) (\theta_{jk} l_k)^{v_{jk}}}{v_{jk}!} \sum_{\alpha_{jk}=0}^{\infty} \frac{(l_k - \theta_{jk} l_k)^{\alpha_{jk}}}{(\alpha_{jk})!} \\ &= \frac{\exp(-l_k) (\theta_{jk} l_k)^{v_{jk}}}{v_{jk}!} \exp(l_k - \theta_{jk} l_k) \\ &= \frac{(\theta_{jk} l_k)^{v_{jk}} \exp(-\theta_{jk} l_k)}{v_{jk}!}\end{aligned}$$

and so  $p(v_{jk}|l_k) \sim \text{Po}(v_{jk}; \theta_{jk} l_k)$ .

Now sum of two independent Poisson distributed variables  $Z = X_1 + X_2$  ( $X_i \sim \text{Po}(x; \lambda_i)$ ) is Poisson distributed:

$$\begin{aligned}p(Z) &= \sum_{x_1=0}^z p(X_1) p(Z - X_1) \\ &= \sum_{x_1=0}^z \frac{\lambda_1^{x_1} e^{-\lambda_1}}{x_1!} \frac{\lambda_2^{z-x_1} e^{-\lambda_2}}{(z-x_1)!} \\ &= \frac{e^{-(\lambda_1+\lambda_2)}}{z!} \sum_{x_1=0}^z \frac{z!}{x_1!(z-x_1)!} \lambda_1^{x_1} \lambda_2^{z-x_1} \\ &= \frac{(\lambda_1 + \lambda_2)^z e^{-(\lambda_1+\lambda_2)}}{z!}\end{aligned}$$

for more by induction.

So  $w_j = \sum_{k=1}^K v_{jk}$  is Poisson distributed:

$$w_j \sim \text{Po}(w_j; \sum_{k=1}^K \theta_{jk} l_k)$$

The joint distribution for  $v_{jk}$  (each is Poisson):

$$\begin{aligned} p(v_{1,k}, v_{2,k} \dots v_{J,k} | l_k, \theta_{jk}) &= \prod_{j=1}^J \frac{(\theta_{jk} l_k)^{v_{jk}} \exp(-\theta_{jk} l_k)}{v_{jk}!} \\ &= e^{-l_k \sum_j \theta_{jk}} l_k^{\sum_j v_{jk}} \prod_j \frac{\theta_{jk}^{v_{jk}}}{v_{jk}!} \quad | \sum_j \theta_{jk} = 1, \sum_j v_{jk} = c_k \\ &= \frac{l_k^{c_k} e^{-l_k}}{c_k!} c_k! \prod_j \frac{\theta_{jk}^{v_{jk}}}{v_{jk}!} \\ &= \text{Po}(c_k; l_k) \times \text{Multinom}(v_{jk}; \theta_{jk}, c_k) \end{aligned}$$

The likelihood of GaP model with latent matrix  $V$  is then

$$\begin{aligned} p(V, l | \alpha, \beta, \theta, K) &= \prod_k p(l_k | \alpha_k, \beta_k) \prod_{jk} p(v_{1k}, v_{2k} \dots v_{J,k} | l_k, \theta_{jk}) \\ &= \prod_k \text{Gamma}(l_k; \alpha_k, \beta_k) \prod_{jk} \text{Po}(c_k; l_k) \times \text{Multinom}(v_{jk}; \theta_{jk}, c_k) \end{aligned}$$

explicitly:

$$p(V, l | \alpha, \beta, \theta, K) = \prod_k \frac{\beta_k^{\alpha_k} l_k^{c_k + \alpha_k - 1} \exp(-(\beta_k + 1)l_k)}{\Gamma(\alpha_k)} \prod_{jk} \frac{\theta_{jk}^{v_{jk}}}{v_{jk}!} \quad (\text{B.2})$$

and

$$\log p(V, l | \alpha, \beta, \theta, K) = \sum_k \left\{ (c_k + \alpha_k - 1) \log l_k - (\beta_k + 1)l_k + \alpha_k \log \beta_k - \log \Gamma(\alpha_k) + \sum_j [v_{jk} \log \theta_{jk} - \log v_{jk}] \right\}$$

$w_j$  is derived from  $V$  so it is not represented.

It is possible to integrate out  $l$  (not sure about discrete values...?):

$$\begin{aligned} p(V | \alpha, \beta, \theta, K) &= \int_0^\infty p(V, l | \alpha, \beta, \theta, K) dl \\ &= \prod_{jk} \frac{\theta_{jk}^{v_{jk}}}{v_{jk}!} \prod_k \frac{\beta_k}{\Gamma(\alpha_k)} \int_0^\infty [l_k^{c_k + \alpha_k - 1} \exp(-(\beta_k + 1)l_k)] dl_k \end{aligned}$$

and

$$\begin{aligned} \int_0^\infty [l_k^{c_k + \alpha_k - 1} \exp(-(\beta_k + 1)l_k)] dl_k &= \int_0^\infty l_k^{z-1} \exp(-(\beta_k + 1)l_k) dl_k \quad | c_k + \alpha_k = z \\ &= \frac{1}{(\beta_k + 1)^z} \int_0^\infty t^{z-1} \exp(-t) dt \quad | (\beta_k + 1)l_k = t \\ &= \frac{1}{(\beta_k + 1)^z} \Gamma(z) \end{aligned}$$



$$p(V|\alpha, \beta, \theta, K) = \prod_k \frac{\beta_k}{(\beta_k + 1)^{c_k + \alpha_k}} \frac{\Gamma(c_k + \alpha_k)}{\Gamma(\alpha_k)} \prod_{jk} \frac{\theta_{jk}^{v_{jk}}}{v_{jk}!}$$

## EM algorithm

The term  $l_k^{(c_k + \alpha_k - 1)} = l_k^{(\sum_j v_{jk} + \alpha_k - 1)}$  in Eq.(B.2) links together  $l_k$  and  $V$  and prevents simple evaluation of  $\mathcal{Q}(\theta, \theta^{\text{old}}) = \mathbb{E}_{p(V, l|\theta^{\text{old}})} [\log p(V, l|\theta, \dots)]$  in the EM algorithm because of the term  $\mathbb{E}_{p(V, l|\theta^{\text{old}})} [v_{jk}]$ . It comes from the Poisson term  $\text{Po}(c_k; l_k)$  in  $p(V, l|\alpha, \beta, \theta, K)$ .

In the likelihood Eq.(B.1) is problematic the term  $w_k \log \sum_k \theta_{jk} l_k$ . (In [Canny, 2004] is the term  $\mathbb{E}_l [\log \sum_k \theta_{jk} l_k]$  approximated by  $\log \mathbb{E}_l [\sum_k \theta_{jk} l_k]$  which might be quite crude.)

## Variational Approximation

Factorised approximate posterior distribution for latent variables:

$$p(l, V|w, \alpha, \beta, \theta, K) \approx q(l, V) = q_l(l)q_V(V)$$

Optimal solution [Bishop, 2006] (p.466 Eq. (10.9))

$$\log q_l^*(l) = \mathbb{E}_{V \sim q_V} [\log p(V, l, w|\theta, \alpha, \beta)] + \text{const} \quad (\text{B.4})$$

$$\log q_V^*(V) = \mathbb{E}_{l \sim q_l} [\log p(V, l, w|\theta, \alpha, \beta)] + \text{const} \quad (\text{B.5})$$

The lower bound is given by [Bishop, 2006] (p.465 Eq. (10.3))

$$\mathcal{L}(q, \theta) = \sum_z q(Z) \log \frac{p(X, Z|\theta)}{q(Z)} = \sum_z q(Z) \log p(X, Z|\theta) + H(q_l) + H(q_V)$$

where

$$\begin{aligned} H(q_l) &= -\mathbb{E}_{l \sim q_l} [\log q_l] \\ H(q_V) &= -\mathbb{E}_{V \sim q_V} [\log q_V] \end{aligned}$$

are the entropy terms.

$$\log p(w|\theta, \alpha, \beta, K) \geq \mathbb{E}_{l, V \sim q(l, V)} [\log p(l, V, w|\theta, \alpha, \beta, K)] + C \quad (\text{B.6})$$

The functional form of the complete likelihood suggests

$$q_l(l) = \prod_k \text{Gamma}(l; \alpha_k, \beta_k) = \prod_k \frac{l_k^{a_k - 1} b_k^{a_k} \exp(-b_k l_k)}{\Gamma(a_k)} \quad (\text{B.7})$$

$$q_V(V) = \prod_{jk} \text{Mutlinom}(v_{jk}; n_{jk}, w_j) = \prod_{jk} \frac{w_j!}{v_{jk}!} n_{jk}^{v_{jk}} \quad (\text{B.8})$$

with  $\sum_k n_{jk} = 1$ .

Then from Eq.(B.4), (B.7) and (B.3) keeping terms dependent on  $l$

$$(a_k - 1) \log l_k - b_k l_k + \text{const} = \left( \sum_j \mathbb{E}_V [v_{jk}] + \alpha_k - 1 \right) \log l_k - (\beta_k + 1) l_k + \text{const}$$

where  $c_k = \sum_j v_{jk}$ . Form Eq.(B.5), (B.8) and (B.3) keeping terms dependent on  $V$

$$v_{jk} \log n_{jk} - \log v_{jk}! + \text{const} = v_{jk} \mathbb{E}_l [\log l_k] + v_{jk} \log \theta_{jk} - \log v_{jk}! + \text{const}$$

so the rewrite rules for the parameters:

$$\begin{aligned}
n_{jk} &= \frac{1}{z_j} \theta_{jk} \exp(\mathbb{E}_l [\log l_k]) \\
a_k &= \sum_j n_{jk} w_j + \alpha_k \\
b_k &= 1 + \beta_k
\end{aligned} \tag{B.9}$$

where  $z_j$  is the normalisation constant ( $\sum_k n_{jk} = 1$ ) so  $z_j = \sum_k \theta_{jk} \exp(\mathbb{E}_l [\log l_k])$  and  $\sum_j \mathbb{E}_V [v_{jk}] = \sum_j n_{jk} w_j$  (Eq.(B.8)).  $\mathbb{E}_{l \sim q_l} [\log l_k] = \psi_0(a_k) - \log b_k$  where  $\psi_0$  is digamma function (logarithmic derivation of the gamma function) and so

$$n_{jk} = \frac{1}{z_j} \theta_{jk} \exp(\psi_0(a_k) - \log b_k)$$

Now recompute model parameter  $\theta$  by maximising lower bound Eq.(B.6) (with constraints  $\sum_j \theta_{jk} = 1$ ). Keeping only term dependent on  $\theta_{jk}$ :

$$\begin{aligned}
\mathcal{L}(\theta) &= \sum_{j,k} \mathbb{E}_{q_V(V)} [v_{jk}] \log \theta_{jk} + \text{const} \\
&= \sum_{j,k} n_{jk} w_j \log \theta_{jk} + \text{const}
\end{aligned}$$

(from Eq.(B.8)  $\mathbb{E}_{q_V(V)} [v_{jk}] = w_j n_{jk}$ )

$$0 = \frac{\partial}{\partial \theta_{mn}} \left[ \sum_{j,k} n_{jk} w_j \log \theta_{jk} + \lambda_n (1 - \sum_p \theta_{pk}) \right]$$

we get

$$\theta_{mn} = \frac{n_{mn} w_m}{\lambda_n}$$

and from normalisation constraints  $\lambda_n = \sum_m n_{mn} w_m$ .

If we take likelihood function over all documents ( $i = 1 : L$ ) each  $w_j \rightarrow w_{j(i)}$  and  $n_{jk} \rightarrow n_{jk(i)}$  then we get

$$\theta_{mn} = \frac{\sum_i n_{mn(i)} w_{m(i)}}{\lambda_n} \tag{B.10}$$

Buntine [Buntine and Jakulin, 2006] even introduce prior on  $\theta_{jk} \sim \text{Dirichlet}(\theta_{jk}; \gamma, J) = C(\gamma_j) \prod_{j=1}^J \theta_{jk}^{\gamma_j - 1}$ . This is incorporated into the complete log-likelihood function  $p(V, l, w, \theta | \alpha, \beta, K)$  so that lower bound  $\mathbb{E}_{l, V \sim q(l, V)} [\log p(l, V, w, \theta | \alpha, \beta, K)]$  and terms dependent on  $\theta$ :

$$\begin{aligned}
\mathcal{L}(\theta) &= \sum_{i,j,k} \mathbb{E}_{q_V(V)} [v_{jk(i)}] \log \theta_{jk} + (\gamma_j - 1) \log \theta_{jk} + \text{const} \\
&= \left( \sum_{i,j,k} n_{jk(i)} w_{j(i)} + \gamma_j - 1 \right) \log \theta_{jk} + \text{const}
\end{aligned}$$

and by maximising with normalisation constraints:

$$\theta_{mn} \propto \sum_i n_{mn(i)} w_{m(i)} + \gamma_j \tag{B.11}$$

The lower bound Eq.(B.6)

$$\begin{aligned}
\mathcal{L}(\theta) &= \mathbb{E}_{l,V \sim q(l,V)} \left[ \sum_k (c_k + \alpha_k - 1) \log l_k - (\beta_k + 1) l_k + \log \frac{\beta_k^{\alpha_k}}{\Gamma(\alpha_k)} + \sum_j [v_{jk} \log \theta_{jk} - \log v_{jk}!] \right] + C \\
&= \sum_k \mathbb{E}_l [\log l_k] (\sum_j \mathbb{E}_V [v_{jk}] + \alpha_k - 1) - (\beta_k + 1) l_k + \log \frac{\beta_k^{\alpha_k}}{\Gamma(\alpha_k)} \\
&\quad + \sum_j [\mathbb{E}_V [v_{jk}] (\log n_{jk} + \log z_j - \mathbb{E}_l [\log l_k] - \mathbb{E}_V [\log v_{jk}!])] + C \\
&= \sum_k \mathbb{E}_l [\log l_k] (\alpha_k - 1) - (\beta_k + 1) l_k + \log \frac{\beta_k^{\alpha_k}}{\Gamma(\alpha_k)} + \sum_j [\mathbb{E}_V [v_{jk}] (\log n_{jk} + \log z_j - \log v_{jk}!)] + C
\end{aligned}$$

where Eq.(B.9) for  $\theta$  was used and  $c_k = \sum_j v_{jk}$  and where  $C = H(q_l) + H(q_V)$  from Eq.(B.6):

$$\begin{aligned}
H(q_l) &= - \sum_k \left\{ (a_k - 1) \mathbb{E}_l [\log l_k] - b_k \mathbb{E}_l [l_k] - \log \frac{b_k^{a_k}}{\Gamma(a_k)} \right\} \\
H(q_V) &= - \sum_{jk} \{ -\mathbb{E}_V [\log v_{jk}!] + \mathbb{E}_V [v_{jk}] \log n_{jk} + \log w_j! \}
\end{aligned}$$

Including these terms we get

$$\mathcal{L} = \sum_k \mathbb{E}_l [\log l_k] (\alpha_k - a_k) + \sum_j w_j \log z_j + \sum_k \log \frac{\Gamma(a_k) \beta_k^{\alpha_k}}{\Gamma(\alpha_k) b_k^{a_k}} - \log \prod_j w_j! \quad (\text{B.12})$$

where Eq.(B.9) for  $b_k$  and  $\sum_k n_{jk} = 1$  was used.

After initialisation the algorithm then repeats until convergence:

1. For each document: update  $n_{jk}$  and  $a_k$  according to Eq.(B.9) (variational E step).
2. Update  $\theta$  according to Eq.(B.10) or (B.11) (variational M step).
3. Compute lower bound on log-probability Eq.(B.12) and check for convergence.

## C Resolution limit for the blinking QDs

### Poisson random variable

This is derivation of the fisher information for Poisson distributed variable  $X$  with mean  $\lambda$ .

$$X \sim \text{Po}(n, \lambda) = p(n|\theta) = \frac{\lambda^n e^{-\lambda}}{n!}$$

Likelihood of the Poisson distributed variable with detection  $n_k$  in  $K$  pixels:

$$l(\theta) = \prod_{k=1}^K l_k = \prod_{k=1}^K \frac{\lambda_k^{n_k} e^{-\lambda_k}}{n_k!} \quad (\text{C.1})$$

where  $l_k(\theta) = p(n_k|\theta)$  to emphasise the dependency on the parameter  $\theta$ .

Log-Likelihood:

$$\mathcal{L} = \sum_k (n_k \log \lambda_k - \lambda_k - \log n_k!)$$

### Fisher Information for a Poisson variable

Fisher information:

$$I(\theta) = -\mathbb{E} \left[ \frac{\partial^2 \mathcal{L}}{\partial \theta^2} \right] = \mathbb{E} \left[ \left( \frac{\partial \mathcal{L}}{\partial \theta} \right)^2 \right] = \mathbb{E} \left[ \left( \sum_k \frac{\partial \log(l_k)}{\partial \theta} \right)^2 \right] = \mathbb{E} \left[ \left( \sum_k \frac{1}{l_k} \frac{\partial l_k}{\partial \theta} \right)^2 \right] \quad (\text{C.2})$$

$$\begin{aligned} I(\theta) &= \mathbb{E} \left[ \left( \sum_k \frac{1}{l_k} \frac{\partial l_k}{\partial \theta} \right) \left( \sum_m \frac{1}{l_m} \frac{\partial l_m}{\partial \theta} \right) \right] \\ &= \mathbb{E} \left[ \sum_k \frac{1}{l_k^2} \left( \frac{\partial l_k}{\partial \theta} \right)^2 \right] + \mathbb{E} \left[ \sum_k \sum_{m \neq k} \frac{1}{l_k} \frac{\partial l_k}{\partial \theta} \frac{1}{l_m} \frac{\partial l_m}{\partial \theta} \right] \end{aligned}$$

as  $n_k$  are iid then the second term can be expressed as

$$\mathbb{E} \left[ \sum_k \sum_{m \neq k} \frac{1}{l_k} \frac{\partial l_k}{\partial \theta} \frac{1}{l_m} \frac{\partial l_m}{\partial \theta} \right] = \sum_k \sum_{m \neq k} \mathbb{E}_k \left[ \frac{1}{l_k} \frac{\partial l_k}{\partial \theta} \right] \mathbb{E}_m \left[ \frac{1}{l_m} \frac{\partial l_m}{\partial \theta} \right]$$

where

$$\mathbb{E}_k [f(n_k)] = \sum_{n_k \geq 0} p(n_k|\theta) f(n_k)$$

But

$$\mathbb{E}_k \left[ \frac{1}{l_k} \frac{\partial l_k}{\partial \theta} \right] = \sum_{n_k} l_k \frac{1}{l_k} \frac{\partial l_k}{\partial \theta} = \sum_{n_k} \frac{\partial l_k}{\partial \theta} = \frac{\partial \sum_{n_k} l_k}{\partial \theta} = 0$$

as  $\sum_{n_k} l_k = \sum_{n_k} p(n_k|\theta) = 1$ . The Fisher Information can then be expressed

$$\begin{aligned} I(\theta) &= \mathbb{E} \left[ \sum_k \frac{1}{l_k^2} \left( \frac{\partial l_k}{\partial \theta} \right)^2 \right] \\ &= \sum_{k=1}^K \sum_{n_k \geq 0} l_k \frac{1}{l_k^2} \left( \frac{\partial l_k}{\partial \theta} \right)^2 \\ &= \sum_{k=1}^K \sum_{n_k \geq 0} \frac{1}{l_k} \left( \frac{\partial l_k}{\partial \theta} \right)^2 \end{aligned}$$

Derivatives of likelihood Eq.(C.1):

$$\frac{\partial l_k}{\partial \theta} = \frac{l_k(n_k - \lambda_k)}{\lambda_k} \frac{\partial \lambda_k}{\partial \theta}$$

And we get:

$$\begin{aligned} I(\theta) &= \sum_{k=1}^k \sum_{n_k \geq 0} \frac{l_k(n_k - \lambda_k)^2}{\lambda_k^2} \left( \frac{\partial \lambda_k}{\partial \theta} \right)^2 \\ &= \sum_{k=1}^k \frac{1}{\lambda_k^2} \left( \frac{\partial \lambda_k}{\partial \theta} \right)^2 \mathbb{E}_k [(n_k - \lambda_k)^2] \end{aligned}$$

for Poisson  $\text{var}(n) = \text{mean}(n) = \lambda$  gives

$$\mathbb{E}_k [(n_k - \lambda_k)^2] = \text{var}(n_k) = \lambda_k$$

and

$$I(\theta) = \sum_{k=1}^K \frac{1}{\lambda_k} \left( \frac{\partial \lambda_k}{\partial \theta} \right)^2 \quad (\text{C.3})$$

This is the pixelised version (detection of the photons in K detectors - CCD camera and  $\lambda_k = \int_{C_k} \lambda(x) dx$  where  $C_k$  is an area of the pixels of the detector).

Non pixelised version [Ram et al., 2006b]s

$$I(\theta) = \int \frac{1}{\lambda(x)} \left( \frac{\partial \lambda(x)}{\partial \theta} \right)^2 dx$$

## Two sources separated by a distance $d$

These are comment on Fisher Information estimation as described in [Ram et al., 2006b].

For two sources separated by a distance  $d$  we have a mean value of the intensity:

$$\lambda = \Lambda_1 f_1 + \Lambda_2 f_2$$

where  $f_i$  and  $\Lambda_i$  is the response function and intensity, respectively, of the source  $i$ . For translationally invariant PSF and in-focus sources:  $f_1 = q(x - \frac{d}{2})$  and  $f_2 = q(x + \frac{d}{2})$

$$\lambda(d) = \Lambda_1 q(x - \frac{d}{2}) + \Lambda_2 q(x + \frac{d}{2})$$

where  $q$  is the PSF of the sources. For pixelised version (integral over pixel area  $C_k$ )

$$\lambda_k(d) = \Lambda_1 \int_{C_k} q(x - \frac{d}{2}) dx + \Lambda_2 \int_{C_k} q(x + \frac{d}{2}) dx$$

so we get (as described in [Ram et al., 2006b])

$$I(d) = \frac{1}{4} \sum_{k=1}^K \frac{\left( \Lambda_1 \int_{C_k} \partial_x q(x - \frac{d}{2}) dx - \Lambda_2 \int_{C_k} \partial_x q(x + \frac{d}{2}) dx \right)^2}{\Lambda_1 \int_{C_k} q(x - \frac{d}{2}) dx + \Lambda_2 \int_{C_k} q(x + \frac{d}{2}) dx} \quad (\text{C.4})$$

**Limit**  $d = 0$  If  $\Lambda_1 = \Lambda_2$  then  $I(d = 0) = 0$  which means  $\text{var}(d = 0) \rightarrow \infty$ . (This does not hold for  $\Lambda_1 \neq \Lambda_2$ ).

**Limit**  $d \rightarrow \infty$  When sources are far apart then the mixing term in nominator in (C.4)  $\Lambda_1 \Lambda_2 \partial_x q(x - \frac{d}{2}) \partial q(d + \frac{d}{2}) = 0$  as the  $\partial_x q(x - \frac{d}{2})$  ( $q(x - \frac{d}{2})$ ) and  $\partial_x q(x + \frac{d}{2})$  ( $q(x + \frac{d}{2})$ ) do not have any overlap. The (C.4) then decomposes into two individual terms (sum of Fisher Information for localisation of individual sources.)

$$\begin{aligned} I(d) &= \frac{1}{4} \sum_{k=1}^K \left[ \frac{\left( \Lambda_1 \int_{C_k} \partial_x q(x - \frac{d}{2}) dx \right)^2}{\Lambda_1 \int_{C_k} q(x - \frac{d}{2}) dx} + \frac{\left( \Lambda_2 \int_{C_k} \partial_x q(x + \frac{d}{2}) dx \right)^2}{\Lambda_2 \int_{C_k} q(x + \frac{d}{2}) dx} \right] \\ &= \frac{1}{4} \sum_{k=1}^K \frac{\left( \int_{C_k} \partial_x q(x) dx \right)^2}{\int_{C_k} q(x) dx} [\Lambda_1 + \Lambda_2] \end{aligned}$$

**Limit**  $\Lambda_i = 0$  If  $\Lambda_1 = 0$  or  $\Lambda_2 = 0$   $I(d) \neq 0$ . So the variance is finite even if one of the sources is not present.

## An alternative way to derive Fisher information for two sources separated by $d$ :

This is a suggestion how to fix the problems with limits for Fisher Information derived above. This gives infinite variance when one of the sources is no present. Also fix weird behaviour of the  $I(d)$  for  $d = 0$ .

For two sources  $f_1 = q(x - c_1)$  and  $f_2 = q(x - c_2)$  we have  $\lambda = \Lambda_1 f_1 + \Lambda_2 f_2$ . The distance between the two sources is  $d = c_1 - c_2$ . This is a linear combination  $\mathbf{a}^T \cdot \mathbf{c}$  of the variable  $\mathbf{c} = (c_1, c_2)$  where  $\mathbf{a} = (1, -1)$ . The variance of  $d$  is given by

$$\text{var}(d) = \text{var}(\mathbf{a}^T \cdot \mathbf{c}) = \mathbf{a}^T \cdot \mathbf{Q} \cdot \mathbf{a} = Q_{11} + Q_{22} - 2Q_{12}$$

where  $\mathbf{Q}$  is a covariance matrix  $\mathbf{Q} = \mathbf{I}^{-1}(\theta)$  and  $\mathbf{I}(\theta)$  is the Fisher information matrix (symmetric  $I_{12} = I_{21}$ )

$$\mathbf{I}(\theta) = \begin{pmatrix} I_{11} & I_{12} \\ I_{12} & I_{22} \end{pmatrix}$$

given by generalisation of Eq.(C.3)

$$I_{ij}(\theta) = \sum_{k=1}^K \frac{1}{\lambda_k} \frac{\partial \lambda_k}{\partial \theta_i} \frac{\partial \lambda_k}{\partial \theta_j}$$

The covariance matrix  $\mathbf{Q}$  is then

$$\mathbf{Q} = \mathbf{I}^{-1}(\theta) = \frac{1}{I_{11}I_{22} - I_{12}^2} \begin{pmatrix} I_{22} & -I_{12} \\ -I_{12} & I_{11} \end{pmatrix}$$

and the variance of  $d = c_1 - c_2$

$$\text{var}(d) = (1, -1)^T \cdot \mathbf{Q} \cdot (1, -1) = \frac{I_{11} + I_{22} + 2I_{12}}{I_{11}I_{22} - I_{12}^2} \quad (\text{C.5})$$

The individual terms of the Fisher Information matrix

$$I_{11} = \sum_{k=1}^K \frac{1}{\lambda_k} \left( \frac{\partial \lambda_k}{\partial c_1} \right)^2 = \sum_{k=1}^K \frac{(\Lambda_1 q'_k(c_1))^2}{\Lambda_1 q_k(c_1) + \Lambda_2 q_k(c_2)}$$

where

$$\begin{aligned} q_k(c) &= \int_{C_k} q(x-c)dx \quad , \quad (q_k(0) = q_k) \\ q'_k(c) &= \int_{C_k} \frac{\partial q(x-c)}{\partial x} dx, \quad (q'_k(0) = q'_k) \end{aligned}$$

If this keeps translational invariance (non-pixelised version does as  $\int_{\mathbb{R}} g(x+c)dx = \int_{\mathbb{R}} g(x)dx$ ) then

$$I_{11} = \sum_{k=1}^K \frac{(\Lambda_1 q'_k)^2}{\Lambda_1 q_k + \Lambda_2 q_k(-d)}$$

where  $d = c_1 - c_2$  and

$$I_{22} = \sum_{k=1}^K \frac{(\Lambda_2 q'_k)^2}{\Lambda_2 q_k + \Lambda_1 q_k(d)}$$

For symmetrical PSF  $q(x-d) = q(x+d)$  we have

$$I_{ii} = \sum_{k=1}^K \frac{(\Lambda_i q'_k)^2}{\Lambda_i q_k + \Lambda_j q_k(d)} \tag{C.6}$$

And the cross term ( $i \neq j$ )

$$I_{ij} = \sum_{k=1}^K \frac{\Lambda_i \Lambda_j q'_k q'_k(d)}{\Lambda_i q_k + \Lambda_j q_k(d)}$$

**Limit**  $d \rightarrow 0$  For  $d = 0$  we have

$$\begin{aligned} I_{ii} &= \frac{\Lambda_i^2}{\Lambda_i + \Lambda_j} S(0) \\ I_{ij} &= \frac{\Lambda_i \Lambda_j}{\Lambda_i + \Lambda_j} S(0) \end{aligned}$$

where  $S(d) = \sum_{k=1}^K \frac{(q'_k)^2}{q_k + q_k(d)}$ .  
Numerator  $p$  in Eq.(C.5)

$$p = I_{11} + I_{22} + 2I_{12} = \frac{S(0)}{\Lambda_1 + \Lambda_2} (\Lambda_1^2 + \Lambda_2^2 + 2\Lambda_1 \Lambda_2) = \frac{S(0)}{\Lambda_1 + \Lambda_2} (\Lambda_1 + \Lambda_2)^2$$

is non-zero for any  $\Lambda_1, \Lambda_2$ .

The denominator in Eq.(C.5)

$$r = \det [\mathbf{I}(\theta)] = I_{11} I_{22} - I_{12}^2 = \frac{S^2(0)}{(\Lambda_1 + \Lambda_2)^2} (\Lambda_1^2 \Lambda_2^2 - (\Lambda_1 \Lambda_2)^2) \equiv 0 \text{ for any } \Lambda_i$$

$\mathbf{I}(\theta)$  is therefore a singular matrix for  $d = 0$  and inversion  $\mathbf{I}^{-1}(\theta)$  does not exist.

However, for the limit  $d \rightarrow 0$  and  $p \neq 0$ ,  $r \rightarrow 0$  and  $\text{var}(d \rightarrow 0) = \frac{p}{r} \rightarrow \infty$ .

**Limit**  $d \rightarrow \infty$  The cross term  $I_{ij} = 0$ ,  $i \neq j$  and we get f

$$\text{var}(d) = \frac{1}{I_{11}} + \frac{1}{I_{22}}$$

and

$$I_{ii} = \sum_{k=1}^K \frac{(\Lambda_i q'_k)^2}{\Lambda_i q_k + \Lambda_j q_k(d)} = \Lambda_i \sum_{k=1}^K \frac{(q'_k)^2}{q_k} = 2\Lambda_i S(0)$$

as the PSF  $q(x)$  (and also  $q'(x)$ ) have a finite support, if  $d$  is big,  $q(x-d)$  is outside the support of the  $q'(x)$ . They have no overlap so it doesn't have any effect in the denominator.

For non-pixelised version,  $\Lambda_1 = \Lambda_2 = \Lambda$  and for Gaussian approximation of the PSF ( $q(x-a) \propto \exp\left(-\frac{(x-a)^2}{2\sigma^2}\right)$  (with  $\sigma = \frac{\sqrt{2}}{2\pi} \frac{\lambda}{NA}$  [Zhang et al., 2007]) we have  $q'(x) = \frac{1}{\sigma^2} x q(x)$  and for  $\Lambda_1 = \Lambda_2 = \Lambda$  and for Gaussian approximation of the PSF  $S(0) = \frac{1}{2\sigma^2}$ :

$$I(d \rightarrow \infty) = \frac{\Lambda}{\sigma^2}$$

$$\text{var}(d \rightarrow \infty) = \frac{\sigma^2}{\Lambda}$$

**Limit**  $\Lambda_i = 0$ ,  $\Lambda_j \neq 0$  then  $I_{ii} \equiv 0$  and  $I_{ij} \equiv 0$  and so  $\det(\mathbf{I}(\theta)) \equiv 0$ , and matrix is singular. In the limit  $\Lambda_i \rightarrow 0$  the variance (C.5)  $\text{var}(d) \rightarrow \infty$ .

## Time distribution of the intensities (blinking)

For likelihood dependent on parameter  $\Lambda_t$  (T different time slices)

$$l_T(d, \Lambda) = \prod_{k=1}^K \prod_{t=1}^T p(n_k|d, \Lambda_t) p(\Lambda_t)$$

$$\mathcal{L}_T(d, \Lambda) = \sum_{k=1}^K \sum_{t=1}^T [\log(l_k(d, \Lambda_t)) + \log(p(\Lambda_t))]$$

as  $p(\Lambda)$  is not dependent on  $d$  then

$$\frac{\partial^2 \mathcal{L}_T(d, \Lambda)}{\partial d^2} = \sum_{t=1}^T \frac{\partial^2 \mathcal{L}(d, \Lambda_t)}{\partial d^2}$$

but in the expectation equation Eq.(C.2) the time dependence appears as

$$I_T(\theta) = -\mathbb{E}_T \left[ \sum_{t=1}^T \frac{\partial^2 \mathcal{L}(d, \Lambda_t)}{\partial d^2} \right] = \sum_{t=1}^T -\mathbb{E}_T \left[ \frac{\partial^2 \mathcal{L}(d, \Lambda_t)}{\partial d^2} \right] = \sum_{t=1}^T \mathbb{E}_T \left[ \left( \frac{\partial \mathcal{L}(d, \Lambda_t)}{\partial d} \right)^2 \right]$$

$$= \sum_{t=1}^T \int_{\Lambda_t} p(\Lambda_t) I(\theta) d\Lambda_t = \sum_{t,k} \int_{\Lambda_t} p(\Lambda_t) \frac{1}{\lambda_k(\Lambda_t)} \left( \frac{\partial \lambda_k(\Lambda_t)}{\partial d} \right)^2 d\Lambda_t$$



## Time distribution of the intensities - integrating out $\Lambda$

$$l_k(d) = \int_{\Lambda} l_k(d, \Lambda) d\Lambda = \int_{\Lambda} p(n_k|d, \Lambda) p(\Lambda) d\Lambda$$

for four state model of two sources:  $\{(\Lambda_1, 0), (0, \Lambda_2), (\Lambda_1, \Lambda_2), (0, 0)\}$ :  $\lambda^1 = \Lambda_1 q(x - c_1)$ ,  $\lambda^2 = \Lambda_2 q(x - c_2)$ ,  $\lambda^3 = +\Lambda_1 q(x - c_1) + \Lambda_2 q(x - c_2)$ ,  $\lambda^4 = 0$  with uniform distribution over these states

$$l_k(\theta) = \frac{1}{4} \sum_{i=1}^4 \text{Po}(\lambda_k^i)$$

derivatives

$$\frac{\partial l_k}{\partial c_p} = \frac{1}{4} \sum_i \frac{\partial \text{Po}(\lambda_k^i)}{\partial c_p} = \frac{1}{4} \sum_i \left( \text{Po}(\lambda_k^i) \frac{(n_k - \lambda_k^i)}{\lambda_k^i} \frac{\partial \lambda_k^i}{\partial c_p} \right)$$

The Fisher information matrix diagonal entries:

$$\begin{aligned} I_{pp}(\theta) &= \mathbb{E} \left[ \left( \sum_{k=1}^N \frac{1}{l_k} \frac{\partial l_k}{\partial c_p} \right)^2 \right] \\ &= \mathbb{E} \left[ \left\{ \sum_{k=1}^N \left( \frac{1}{\sum_{j=1}^4 \text{Po}(\lambda_k^j)} \frac{\partial \sum_{i=1}^4 \text{Po}(\lambda_k^i)}{\partial c_p} \right) \right\} \left\{ \sum_{l=1}^N \left( \frac{1}{\sum_{j=1}^4 \text{Po}(\lambda_l^j)} \frac{\partial \sum_{i=1}^4 \text{Po}(\lambda_l^i)}{\partial c_p} \right) \right\} \right] \\ &= \sum_{k=1}^N \mathbb{E}_k \left[ \frac{\left( \sum_{i=1}^4 \frac{\partial \text{Po}(\lambda_k^i)}{\partial c_p} \right)^2}{\left( \sum_{j=1}^4 \text{Po}(\lambda_k^j) \right)^2} \right] \end{aligned} \quad (\text{C.7})$$

as the cross terms  $(k, l)$  in the sum (2nd row) are zeros:

$$\begin{aligned} \mathbb{E} \left[ \left( \frac{\sum_{i=1}^4 \frac{\partial \text{Po}(\lambda_k^i)}{\partial c_p}}{\sum_{j=1}^4 \text{Po}(\lambda_k^j)} \right) \left( \frac{\sum_{i=1}^4 \frac{\partial \text{Po}(\lambda_l^i)}{\partial c_p}}{\sum_{j=1}^4 \text{Po}(\lambda_l^j)} \right) \right] &= \mathbb{E}_k \left[ \frac{\sum_{i=1}^4 \frac{\partial \text{Po}(\lambda_k^i)}{\partial c_p}}{\sum_{j=1}^4 \text{Po}(\lambda_k^j)} \right] \mathbb{E}_l \left[ \frac{\sum_{i=1}^4 \frac{\partial \text{Po}(\lambda_l^i)}{\partial c_p}}{\sum_{j=1}^4 \text{Po}(\lambda_l^j)} \right] \\ &= \sum_{i=1}^4 \frac{\partial}{\partial c_p} \left( \sum_{n_k \geq 0} \text{Po}(\lambda_k^i) \right) \sum_{i=1}^4 \frac{\partial}{\partial c_p} \left( \sum_{n_l \geq 0} \text{Po}(\lambda_l^i) \right) \\ &= 0 \end{aligned}$$

Expressing the derivatives and the expectation from Eq.(C.7):

$$\begin{aligned} I_{pp}(\theta) &= \sum_{k=1}^N \mathbb{E}_k \left[ \left\{ \frac{\sum_{i=1}^4 \left( \text{Po}(n_k; \lambda_k^i) \frac{(n_k - \lambda_k^i)}{\lambda_k^i} \frac{\partial \lambda_k^i}{\partial c_p} \right)}{\sum_{j=1}^4 \text{Po}(n_k; \lambda_k^j)} \right\}^2 \right] \\ &= \frac{1}{4} \sum_{k=1}^N \sum_{n_k \geq 0} \frac{\left\{ \sum_{i=1}^4 \left( \text{Po}(n_k; \lambda_k^i) \frac{(n_k - \lambda_k^i)}{\lambda_k^i} \frac{\partial \lambda_k^i}{\partial c_p} \right) \right\}^2}{\sum_{j=1}^4 \text{Po}(n_k; \lambda_k^j)} \end{aligned}$$

For the four states model we have  $\lambda^3(c_1, c_2) = \lambda^1(c_1) + \lambda^2(c_2)$  and so  $\frac{\partial \lambda^3}{\partial c_p} = \frac{\partial \lambda^p}{\partial c_p}$  and  $\frac{\partial \lambda^j}{\partial c_p} = 0$ ,  $i \neq j$  for  $p = \{1, 2\}$ ,  $j = \{1, 2, 4\}$ ; so

$$I_{pp}(\theta) = \sum_{k=1}^N \left( \frac{\partial \lambda_k^p}{\partial c_p} \right)^2 \mathbb{E}_k \left[ \left\{ \frac{\sum_{i=\{p,3\}} \left( \text{Po}(n_k; \lambda_k^i) \frac{(n_k - \lambda_k^i)}{\lambda_k^i} \right)}{\sum_{j=1}^4 \text{Po}(n_k; \lambda_k^j)} \right\}^2 \right]$$

The Fisher information matrix off-diagonal entries:

$$\begin{aligned}
I_{pq}(\theta) &= \sum_{k=1}^N \mathbb{E}_k \left[ \frac{\left( \sum_{i=1}^4 \frac{\partial \text{Po}(\lambda_k^i)}{\partial c_p} \right) \left( \sum_{l=1}^4 \frac{\partial \text{Po}(\lambda_k^l)}{\partial c_q} \right)}{\left( \sum_{j=1}^4 \text{Po}(\lambda_k^j) \right)^2} \right] \\
&= \sum_{k=1}^N \left( \frac{\partial \lambda_k^p}{\partial c_p} \right) \left( \frac{\partial \lambda_k^q}{\partial c_q} \right) \mathbb{E}_k \left[ \frac{\left( \sum_{i=\{p,3\}} \text{Po}(n_k; \lambda_k^i) \frac{(n_k - \lambda_k^i)}{\lambda_k^i} \right) \left( \sum_{i=\{q,3\}} \text{Po}(n_k; \lambda_k^i) \frac{(n_k - \lambda_k^i)}{\lambda_k^i} \right)}{\left( \sum_{j=1}^4 \text{Po}(n_k; \lambda_k^j) \right)^2} \right]
\end{aligned} \tag{C.8}$$

**Limit**  $d \rightarrow 0$  When  $c^1 = c^2$  then  $\lambda^1 = \lambda^2$  and  $\frac{\partial \text{Po}(\lambda^1)}{\partial c^1} = \frac{\partial \text{Po}(\lambda^2)}{\partial c^2}$ . Then all entries in  $I_{pq}$  are equal and the matrix is singular. For the limit  $d \rightarrow 0$  the determinanat  $\det(\mathbf{I}) \rightarrow 0$  and the variance  $\text{var}(d) \rightarrow \infty$ .

**Limit**  $d \rightarrow \infty$  Sources are far apart and  $\lambda^1$  and  $\lambda^2$  do not have a common overlap. For  $k'$  where  $\lambda_{k'}^1 > 0$ ,  $\lambda_{k'}^2 \equiv 0$  and  $\text{Po}(n_{k'}, \lambda_{k'}^3) = \text{Po}(n_{k'}, \lambda_{k'}^1) + \text{Po}(n_{k'}, \lambda_{k'}^2 = 0) = \text{Po}(n_{k'}, \lambda_{k'}^1) + 1$ . Also  $\frac{\partial \lambda^p}{\partial c_q} = 0$ ,  $p \neq q$ . From Eq.(C.7) the diagonal elements

$$\begin{aligned}
I_{pp} &= \sum_{k=1}^N \mathbb{E}_k \left[ \frac{\left( 2 \frac{\partial \text{Po}(\lambda_k^p)}{\partial c_p} \right)^2}{(2\text{Po}(\lambda_k^p) + 2\text{Po}(\lambda_k^q))^2} \right] \\
&= \sum_{k=1}^N \mathbb{E}_k \left[ \frac{\left( \text{Po}(\lambda_k^p) \frac{(n_k - \lambda_k^p)^2}{\lambda_k^p} \frac{\partial \lambda_k^p}{\partial c_p} \right)^2}{(\text{Po}(\lambda_k^p) + 1)^2} \right] \\
&= \sum_{k=1}^N \left( \frac{1}{\lambda_k^p} \frac{\partial \lambda_k^p}{\partial c_p} \right)^2 \mathbb{E}_k \left[ (n_k - \lambda_k^p)^2 \left( \frac{\text{Po}(\lambda_k^p)}{\text{Po}(\lambda_k^p) + 1} \right)^2 \right]
\end{aligned}$$

For large  $\lambda_k^p$  the second term in the expectation is approximately one:  $\frac{\text{Po}(\lambda_k^p)}{\text{Po}(\lambda_k^p) + 1} = 1 - \frac{1}{1 + \text{Po}(\lambda_k^p)} \approx 1$

$$I_{pp} \approx \frac{1}{2} \sum_{k=1}^N \frac{1}{\lambda_k^p} \left( \frac{\partial \lambda_k^p}{\partial c_p} \right)^2 \tag{C.9}$$

which is the Eq.(C.3) (up to the factor 2). As the the term is upper bounded by one:  $\frac{\text{Po}(\lambda_k^p)}{\text{Po}(\lambda_k^p) + 1} = 1 - \frac{1}{1 + \text{Po}(\lambda_k^p)} < 1$  the terms  $I_{pp}$  will be slightly smaller then the approximation Eq.(C.9):

$$I_{pp} = \frac{1}{2} \sum_{k=1}^N \frac{1}{\lambda_k^p} \left( \frac{\partial \lambda_k^p}{\partial c_p} \right)^2 - \epsilon \tag{C.10}$$

The off-diagonal entries:

$$I_{pq} = 0$$

as

$$\frac{\partial \text{Po}(\lambda^p)}{\partial c_p} \frac{\partial \text{Po}(\lambda^q)}{\partial c_q} = 0$$

because  $\lambda^p(x)$  and  $\lambda^q(x)$  do not have a common support. and the

Therefore

$$\begin{aligned}
\text{var}(d) &= \frac{1}{I_{11}} + \frac{1}{I_{22}} \\
&= 2 \left( \frac{1}{I_{11}^{\text{static}} - \epsilon} + \frac{1}{I_{22}^{\text{static}} - \epsilon} \right) \\
&> 2\text{var}(d^{\text{static}})
\end{aligned} \tag{C.11}$$

where  $I^{\text{static}}$  and  $\text{var}^{\text{static}}$  correspond to the Fisher information matrix Eq.(C.3) and the variance Eq.(C.5) of the static case. The factor of 2 stems from the fact that the total number of photons is double in the static case compared to the blinking model.